Characterizing Decentralized Wireless Networks with Temporal Correlation in the Low Outage Regime

Kapil Gulati, *Member, IEEE,* Radha Krishna Ganti, *Member, IEEE,* Jeffrey G. Andrews, *Senior Member, IEEE,* Brian L. Evans, *Fellow, IEEE,* and Srikathyayani Srikanteswara, *Member, IEEE*

***Abstract*—Communication in decentralized wireless networks is limited by interference. Because transmissions typically last for more than a single contention time slot, interference often exhibits a strong statistical dependence over time that results in temporally correlated communication performance. The temporal dependence in interference increases as user mobility decreases and/or the total transmission time increases. We propose a network model that spans the extremes of temporal independence to long-term temporal dependence. Using the proposed model, closed-form single hop communication performance metrics are derived that are asymptotically exact in the low outage regime. The primary contributions are (i) deriving the joint temporal statistics of network interference and showing that it follows a multivariate symmetric alpha stable distribution; (ii) utilizing the joint interference statistics to derive closed-form expressions for local delay, throughput outage probability, and average network throughput; and (iii) using the joint interference statistics to redefine and analyze the network transmission capacity that captures the throughput-delay-reliability tradeoffs in single hop transmissions. Simulation results verify the closed-form expressions derived in this paper and we demonstrate up to $2\times$ gain in network throughput and reliability by optimizing certain parameters of medium access control layer protocol in view of the temporal correlations.**

***Index Terms*—Co-channel interference, decentralized networks, outage probability, temporal correlation, transmission capacity.**

I. Introduction

Characterizing the communication performance of single hop transmissions from a transmitter to its next hop receiver is a fundamental step towards understanding the end-to-end performance of multihop wireless networks. Over the last decade, significant research has been done towards analyzing the single hop communication performance in a decentralized wireless network, such as a wireless ad hoc network, under the assumption that user locations at any given time instant follow a spatial Poisson point process (PPP) [2], [3]. Key measures of communication performance include outage probability [3], transmission capacity [4], and local delay [5], [6]. Such measures are affected not only by the user locations at any given time instant, but also the correlation in user locations over time [7]. Much of the prior work assumes either no dependence or complete correlation in the user locations over time [4]–[6]. This captures only the extremes of either no mobility and infinitely backlogged user queues (complete correlation), or highly mobile users and/or short user queues (little or no correlation). In many realistic settings, however, there is some mobility or traffic bursts that play out over a significantly slower time scale than contention and channel access. It is therefore important to study the throughput, delay, and reliability of single hop transmissions when there is nontrivial correlation in the transmitter locations.

A. Motivation and Prior Work

Temporal correlation in user locations, and hence temporal dependence in interference, depends on user mobility and the typical duration of user transmissions. Modeling nontrivial correlation in user locations thus captures the random mobility and random queue size of users in a decentralized network. Much of the prior work, however, assumes temporal independence in user locations – primarily for mathematical tractability [4], [8]. Extensions for complete temporal correlation, as an effect of no user mobility and infinitely backlogged user queues, was recently studied in [5], [6]. In [5], [6], the local delay in networks with both static (no user mobility) and highly mobile networks (high user mobility) was characterized. Local delay was defined as the mean time required for a successful transmission from a transmitter to its next hop receiver. With complete temporal correlation, local delay captures the effect of temporal dependence in interference on the throughput of single hop transmissions. With nontrivial correlations, however, the local delay measure alone captures only the first-success rate since consecutive transmission successes are no longer statistically identical. In this paper, we first propose a network that spans the extremes of temporal independence to long-term temporal dependence in interference. The proposed network model is then used to define and characterize performance measures that entirely capture the throughput-delay-reliability tradeoffs in single hop transmissions.

Manuscript submitted May 26, 2011; revised Oct. 27, 2011; Apr. 19, 2012; accepted Apr. 20, 2012.

This research was supported by Intel Corporation and DARPA ITMANET (R. K. Ganti and J. G. Andrews). This research is a part of the first author's Ph.D. dissertation [1], and was carried out at The University of Texas at Austin, Austin, TX 78712, USA.

K. Gulati is with Qualcomm Incorporated, San Diego, CA 92121, USA (e-mail: gulati.k@gmail.com).

R. K. Ganti is with The Indian Institute of Technology Madras, Chennai 600036, India (e-mail: rganti@ee.iitm.ac.in)

J. G. Andrews and B. L. Evans are with Wireless Networking and Communications Group, The University of Texas at Austin, TX 78712, USA (e-mail: {jandrews, bevans}@ece.utexas.edu).

S. Srikanteswara is with Intel Corporation, Santa Clara, CA 95054, USA (e-mail: srikathyayani.srikanteswara@intel.com).

Although we describe the system model with respect to the duration of user transmissions, it can also be interpreted with respect to the varying user mobility. A user may start a transmission at any time, termed as the *emerging time*, and the transmissions lasts for a random duration, termed as the *lifetime*. Distribution of the random lifetime of users can be deduced from typical data transfer characteristics in the network. Thus at any given time, users that transmit include those whose transmissions are ongoing from some time in the past, and users that just started transmitting. Hence, the temporal dependence in the interference increases as the lifetime of a typical user increases. The static and highly mobile network models studied in prior work are included as special cases in this network model by appropriately choosing the lifetime distribution and constraints on the emerging time of users.

The paper adopts a novel approach to derive the single hop communication performance measures in closed-form. Much of the prior work formulates the system model as an abstraction of transmit and receive power, uses tools from stochastic geometry, and attempts to express the measures of communication performance in terms of the Laplace transform of interference [2], [3], [9]. The performance measures can typically be derived in closed-form only under the assumption of Rayleigh fading. Further, to the best of our judgment, using prior methods to derive closed-form expressions for the performance measures considered in this paper is hard. In contrast, we formulate the problem as an abstraction of amplitude and phase of the interfering and desired signals, and express the performance measures in terms of the joint tail probability of the interference. The joint tail probabilities are arrived at by first deriving the joint characteristic function of interference in a known statistical form. An advantage of this approach is that we do not require stringent assumptions on the fading distribution [10]. The disadvantage of this approach is that our results are mathematically exact only in the low outage probability regime. We assume a low outage regime to derive a closed-form expression for the joint tail probability, and also the joint characteristic function for non-Rayleigh fading. However, the results match closely in simulations even when the outage probability is fairly high.

Under the assumptions of PPP distributed user locations and a power-law pathloss function, the interference statistics at any given time instant follow a symmetric alpha stable distribution [10]–[16]. Further, under additional restrictive assumptions on the user emission and fading distributions, the joint temporal statistics of interference follow a multidimensional symmetric alpha stable distribution [13], [14]. To the best of our knowledge, in lieu of the restrictive assumptions on user emission and fading distributions, the closed-form joint temporal statistics of interference for the network model considered in this paper cannot be derived using prior results. Further, even when temporal interference exactly follows a multidimensional symmetric alpha stable distribution, the closed-form tail probability expressions required for deriving the single hop communication performance measures considered in this paper are not known.

TABLE I: Summary of Notation

Symbol	Description
$\mathbf{\Pi}^{(m)}$	Poisson point process of emerging nodes at time slot m
$\lambda^{(m)}$	intensity of $\mathbf{\Pi}^{(m)}$
$\mathbf{\Xi}_n(\mathbf{\Xi}_{k,n})$	point process of active nodes at slot n (that emerged at slot k)
$\mathbf{R}, \mathbf{R}^{(m)}$	(random) location of a node in space
$\mathbf{L}, \mathbf{L}^{(m)}$	(random) time slots a node transmits (i.e., lifetime)
γ	power pathloss exponent ($\gamma > 2$)
$\mathbf{X} = \mathbf{B}e^{j\boldsymbol{\phi}}$	amplitude and phase of interferer emissions
$\mathbf{g} = \mathbf{h}e^{j\boldsymbol{\theta}}$	amplitude and phase of fast fading
$\mathbf{I}_n(\mathbf{I}_{k,n})$	interference at slot n (due to nodes that emerged at slot k)
$\overline{\mathbf{I}}_{k,1:n}$	$\triangleq \left\{\mathbf{I}_{k,1}^{(I)}, \mathbf{I}_{k,1}^{(Q)}, \cdots, \mathbf{I}_{k,n}^{(I)}, \mathbf{I}_{k,n}^{(Q)}\right\}$, $\mathbf{I}_{k,m}$=$\mathbf{I}_{k,m}^{(I)}$+$j\mathbf{I}_{k,m}^{(Q)}$
$\overline{\omega}_{1:n}$	$\triangleq \left\{\omega_1^{(I)}, \omega_1^{(Q)}, \cdots, \omega_n^{(I)}, \omega_n^{(Q)}\right\}$ frequency variables
$\mathbf{\Phi}_{\overline{\mathbf{I}}}(\overline{\omega}_{1:n})$	characteristic function of $\overline{\mathbf{I}}$, where $\overline{\mathbf{I}}$ = $\overline{\mathbf{I}}_{k,n}$ or $\overline{\mathbf{I}}_n$
$\psi_{\overline{\mathbf{I}}}(\overline{\omega}_{1:n})$	log-characteristic function of $\overline{\mathbf{I}}$, where $\overline{\mathbf{I}}$ = $\overline{\mathbf{I}}_{k,n}$ or $\overline{\mathbf{I}}_n$
Δ	(random) number of consecutive failed transmissions
$\mathbf{S}(n)$	(random) number of successes in n time slots
$\mathtt{LD}, \mathtt{C}^{\mathtt{av}}$	local delay, average network throughput
$\overline{\mathbf{L}}, \epsilon$	average lifetime, throughput outage constraint
$\mathtt{TC}(\overline{\mathbf{L}}, \epsilon)$	transmission capacity
D	distance between a transmitter-receiver pair
T	signal-to-interference ratio threshold for detection success
S_d	unit sphere in d dimensions
α	characteristic exponent of alpha stable vector, $\alpha = 4/\gamma$
$\overline{\Gamma}$	spectral measure of symmetric alpha stable vector
σ	dispersion of an isotropic symmetric alpha stable vector
$\mathcal{F}_{\mathbf{L}}(\cdot), K(\cdot)$	constants defined in (26) and (31), respectively
$\mathcal{M}_{\mathbf{L}}(\cdot), \mathcal{N}(\cdot)$	constants defined in (38) and (40), respectively

B. Contribution, Organization, and Notation

To characterize the single hop communication performance, we first derive the joint temporal statistics of interference that capture the effect of temporal correlation in user locations. We show that in the low outage regime, the joint characteristic function of interference follows a multivariate symmetric alpha stable distribution for any general user emission and fading distributions. The joint characteristic function is exact when the amplitude of the faded interferer emissions are Rayleigh distributed, and closely characterizes the tail probability of interference otherwise. Using properties of the multivariate symmetric alpha stable distribution, we provide new theorems for expressing the joint tail probability of interference in closed-form. The closed-form expressions of tail probability enable us to derive the following single hop communication performance measures: (i) local delay, (ii) throughput outage probability, (iii) average network throughput, and (iv) transmission capacity. Transmission capacity for single hop transmissions was first defined for temporally independent user locations as the maximum allowable density of transmitting users satisfying an outage probability constraint [4], [8]. In this paper, we extend the definition of transmission capacity to account for temporal dependence and show that it captures the throughput-delay-reliability tradeoff of single hop transmissions. Using the extended definition, we demonstrate up to $2\times$ gain in network throughput and reliability by optimizing over the lifetime distribution – which motivates designing MAC protocols to incorporate the effect of temporal correlation.

The paper is organized as follows. Section I-B discusses the system model. Section III derives joint interference statistics, including characteristic function and tail probability, for the two network models discussed in the system model. Section

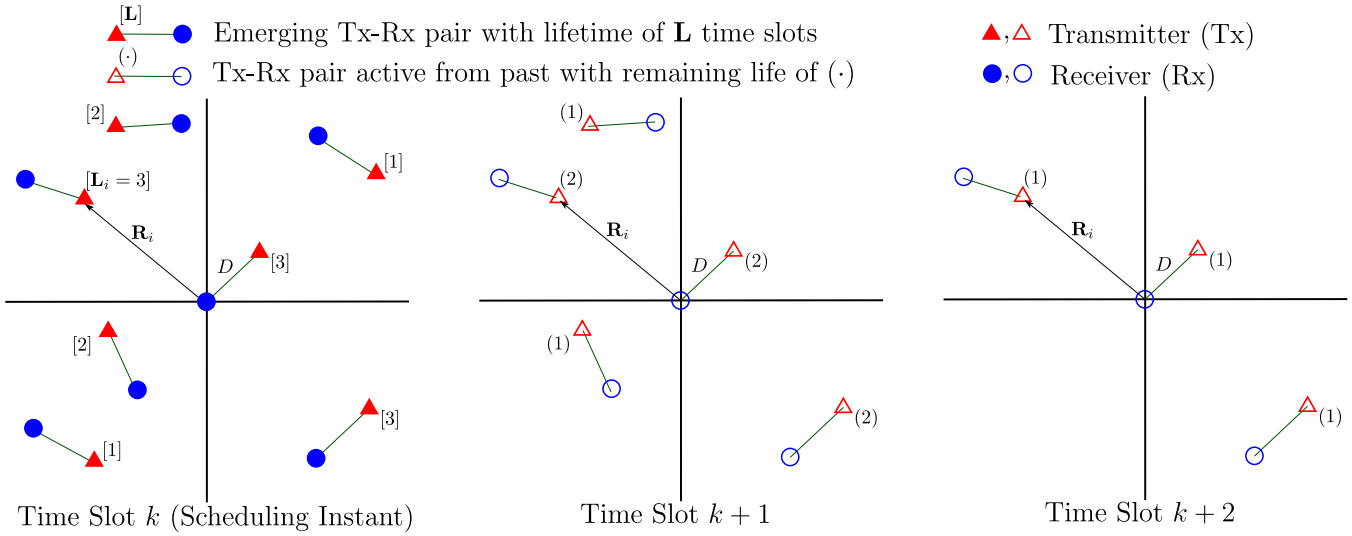

Fig. 1: Network Model I: nodes emerge only at fixed time slots and transmit for a random number of time slots (= $\mathbf{L}$).

IV uses the results on tail probability to derive various single hop communication performance measures. Section V presents the numerical simulation results to corroborate our claims. Appendix A contains a brief overview of statistical properties of symmetric alpha stable vectors and proofs for the new theorems used in the paper. Throughout this paper, random variables are represented using boldface notation and deterministic parameters are represented using non-boldface type. Table I summarizes the notation used in this paper.

II. System Model

Time is slotted at the symbol time scale. The locations of transmitters, also referred to as nodes, are modeled using a spatial point process. A node is said to *emerge* at a particular time slot if it first starts to transmit at that time slot. All nodes transmitting at a given time slot are referred to as *active* nodes at that time slot. Thus at each time slot n, the set of active nodes is a union over the sets of nodes that first emerged at a slot $m \leq n$ and are still active at the time slot n. Emerging nodes at any time slot m are assumed to be spatially distributed according to a homogeneous PPP $\mathbf{\Pi}^{(m)} = \left\{\left(\mathbf{R}_i^{(m)}, \mathbf{L}_i^{(m)}\right), i \geq 1\right\}$ with intensity $\lambda^{(m)}$. Here $\mathbf{R}_i^{(m)}$ is the random location of the node i that first emerged at time m, and $\mathbf{L}_i^{(m)} \geq 1$ is the random number of time slots (lifetime) it intends to be active. Each node is assumed to be associated with a distinct receiver at a distance D in a random direction. Extension to include randomness in D is straightforward [4]. A node may intend to transmit single or multiple packets in its lifetime, and may not be successful due to packet errors. We consider two network models – network model I represents a synchronous network where nodes emerge only at fixed time slots, while network model II represents a asynchronous network where nodes may emerge at any time slot.

A. Network Model I: Synchronous

Consider a network, as depicted in Fig. 1, in which the nodes can start transmitting only at fixed time slots, referred to as MAC scheduling instants. The MAC scheduling instants are spaced apart by $L_{max}+1$ time slots such that all nodes complete their transmission prior to the next scheduling instant. For analysis of such a network, we consider just one MAC scheduling cycle. Thus we can model the interference by assuming that nodes emerge only at the time slot k with $\lambda^{(k)} = \lambda$, $\lambda^{(m)} = 0$ for $m \neq k$, and $\mathbb{P}\left(\mathbf{L}^{(k)} \leq L_{max}\right) = 1$ for all nodes. Further, without loss of generality, $k = 1$ could be chosen for analysis of the network. However, we keep k as a variable so that it can be used as a building block for network model II.

The point process of active nodes at any time slot $n \geq k$ is a subset of the point process $\mathbf{\Pi}^{(k)}$, and can be expressed as $\mathbf{\Xi}_{k,n} = \left\{\mathbf{R} : (\mathbf{R}, \mathbf{L}) \in \mathbf{\Pi}^{(k)}, \mathbf{L} \geq n-k+1\right\}$. For $n < k$, $\mathbf{\Xi}_{k,n}$ is an empty set since no nodes have yet emerged. Since the underlying node distribution follows a PPP, by Slivnyak's theorem and the random translation invariance property of PPP, we can add a typical transmit node to the point process such that its associated receiver lies on the origin without affecting the node distribution [2]. Note that the active node distribution at any given time instant $n \geq k$ is a PPP with intensity $\lambda\mathbb{P}\left(\mathbf{L} \geq n-k+1\right)$. The node distribution, however, is correlated across time slots. Complete temporal correlation is a special case of network model I with $\mathbf{L} \xrightarrow{p} \infty$.

The sum interference $\mathbf{I}_{k,n}$ observed at the typical receiver located at the origin at the time slot n due to the nodes that emerged at time slot k can then be represented as [10]

$$\mathbf{I}_{k,n} = \sum_{\mathbf{R}_i \in \mathbf{\Xi}_{k,n}} \mathbf{r}_i^{-\frac{\gamma}{2}} \mathbf{h}_i(n) \mathbf{B}_i(n) e^{j(\boldsymbol{\phi}_i(n) + \boldsymbol{\theta}_i(n))} \tag{1}$$

where i is the interferer index, $\mathbf{r}_i = \|\mathbf{R}_i\|$ are the random distances of active interferers from the receiver, γ is the power pathloss exponent, $\mathbf{B}_i(n)e^{j\boldsymbol{\phi}_i(n)}$ are the narrowband emissions from interferer i at time slot n, and $\mathbf{h}_i(n)e^{j\boldsymbol{\theta}_i(n)}$ are the distortions due to fast fading experienced by the interferer emissions. Random variables $\mathbf{B}_i(n), \mathbf{h}_i(n), \boldsymbol{\phi}_i(n), \boldsymbol{\theta}_i(n)$ are each assumed to be *i.i.d.* for each interferer i and time slot n. At the symbol time scale, the random amplitude and phase are

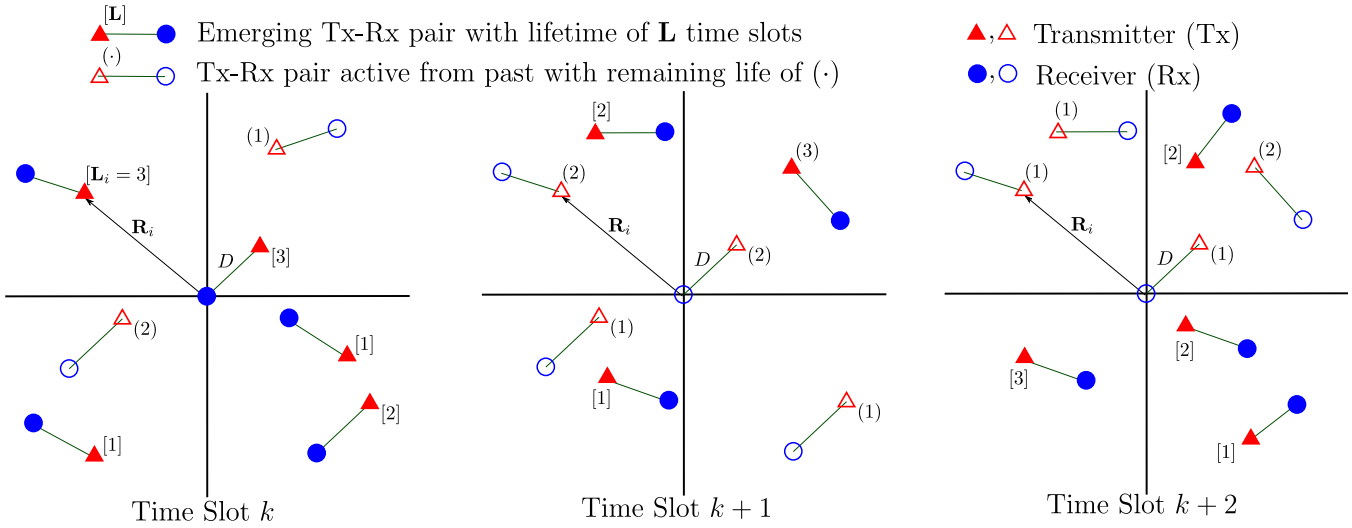

Fig. 2: Network Model II: nodes can emerge at any time slot and are active for a random number of time slots ($= \mathbf{L}$).

typically uncorrelated over time, but may still be temporally dependent. The assumption of temporally *i.i.d.* amplitude and phase, however, is made for mathematical tractability and does not affect the large scale trends in the results. Assuming the actual emerging time of the interferers to be uniformly distributed between two time slots, $\boldsymbol{\phi}_i(n)$ and $\boldsymbol{\theta}_i(n)$ can be assumed to be uniformly distributed on $[0, 2\pi]$.

The signal-to-interference ratio (SIR) at the typical receiver at time slot n can be expressed as

$$\begin{aligned}\mathtt{SIR}_{k,n} &= \frac{\left\|D^{-\frac{\gamma}{2}}\mathbf{h}_0(n)\mathbf{B}_0(n)e^{j(\boldsymbol{\phi}_0(n)+\boldsymbol{\theta}_0(n))}\right\|^2}{\left\|\mathbf{I}_{k,n}\right\|^2} \\ &= \frac{D^{-\gamma}\mathbf{h}_0^2(n)\mathbf{B}_0^2(n)}{\left\|\mathbf{I}_{k,n}\right\|^2} \end{aligned} \tag{2}$$

where $\mathbf{B}_0(n)e^{j(\boldsymbol{\phi}_0(n))}$ is the random emission and $\mathbf{h}_0(n)e^{j(\boldsymbol{\theta}_0(n))}$ is random fading at time slot n corresponding to the desired transmitter-receiver pair.

B. Network Model II: Asynchronous

Model II, as depicted in Fig. 2, extends the network model I by removing the assumption of globally synchronized MAC scheduling instants. This represents a fully decentralized wireless network where the nodes can emerge at any time slot and stay active for a random number of slots. The point process for the emerging nodes $\boldsymbol{\Pi}^{(m)}$ is assumed to be independent and identical over the time slots m with $\lambda^{(m)} = \lambda$, $\forall m$. The point process of active nodes $\boldsymbol{\Xi}_n$ is thus a stationary process.

The point process of active nodes at time slot n can be represented as a union over the active node point process for network model I, given as $\boldsymbol{\Xi}_n = \bigcup_{k=-\infty}^{n} \boldsymbol{\Xi}_{k,n}$. Similar to network model I, we can add a typical node to the point process of active nodes such that its associated receiver lies on the origin without affecting the node distribution. Note that the active node distribution at any given time instant n is a PPP with intensity $\lambda \sum_{k=-\infty}^{n} \mathbb{P}\left(\mathbf{L} \geq n-k+1\right) = \lambda\mathbb{E}\{\mathbf{L}\}$. The node distribution is correlated across time slots unless $\mathbb{P}\left(\mathbf{L}^{(k)} = 1\right) = 1$ for all nodes and time slots k. Temporal independence is thus a special case of network model II with $\mathbf{L} \overset{p}{=} 1$.

Since $\boldsymbol{\Xi}_n = \bigcup_{k=-\infty}^{n} \boldsymbol{\Xi}_{k,n}$, the sum interference at the typical receiver located at the origin from all active interfering nodes at time slot n can be expressed as

$$\begin{aligned}\mathbf{I}_n &= \sum_{k=-\infty}^{n} \mathbf{I}_{k,n} \\ &= \sum_{k=-\infty}^{n} \left[\sum_{\mathbf{R}_i \in \boldsymbol{\Xi}_{k,n}} \mathbf{r}_i^{-\frac{\gamma}{2}}\mathbf{h}_i(n)\mathbf{B}_i(n)e^{j(\boldsymbol{\phi}_i(n)+\boldsymbol{\theta}_i(n))}\right]. \end{aligned} \tag{3}$$

The signal-to-interference ratio (SIR) at the typical receiver at time slot n can be expressed as

$$\begin{aligned}\mathtt{SIR}_{n} &= \frac{\left\|D^{-\frac{\gamma}{2}}\mathbf{h}_0(n)\mathbf{B}_0(n)e^{j(\boldsymbol{\phi}_0(n)+\boldsymbol{\theta}_0(n))}\right\|^2}{\left\|\mathbf{I}_{n}\right\|^2} \\ &= \frac{D^{-\gamma}\mathbf{h}_0^2(n)\mathbf{B}_0^2(n)}{\left\|\mathbf{I}_{n}\right\|^2}. \end{aligned} \tag{4}$$

III. Joint Statistics of Interference

In this section, we derive the joint temporal statistics of interference for network models I and II. The properties of the joint temporal statistics of interference are then used to derive closed-form expressions for the joint tail probability of interference over time.

A. Network Model I

Let $\bar{\mathbf{I}}_{k,1:n} = \left\{\mathbf{I}_{k,1}^{(I)}, \mathbf{I}_{k,1}^{(Q)}, \mathbf{I}_{k,2}^{(I)}, \mathbf{I}_{k,2}^{(Q)}, \cdots, \mathbf{I}_{k,n}^{(I)}, \mathbf{I}_{k,n}^{(Q)}\right\}$ denote the vector of the in-phase and quadrature phase components of interference at time slots 1 through n due to nodes that emerged at time instant k, where $\mathbf{I}_{k,n}$ is given by (1). Further, let $\overline{\omega}_{1:n} = \left\{\omega_1^{(I)}, \omega_1^{(Q)}, \omega_2^{(I)}, \omega_2^{(Q)}, \cdots, \omega_n^{(I)}, \omega_n^{(Q)}\right\}$ denote the vector of frequency variables. To derive the joint statistics, we consider the nodes to be distributed over a disc of radius R, denoted as $b(0, R)$, and take the limit on the joint distribution

as $R \to \infty$. Using (1), the joint characteristic function of $\overline{\mathbf{I}}_{k,1:n}$ can be expressed as

$$\begin{aligned}
&\boldsymbol{\Phi}_{\overline{\mathbf{I}}_{k,1:n}}(\overline{\omega}_{1:n}) \\
&= \mathbb{E}\Bigg\{\exp\Bigg(j\sum_{m=1}^{n}|\omega_m| \sum_{(\mathbf{R}_i,\mathbf{L}_i)\in\boldsymbol{\Pi}^{(k)}} \mathbf{r}_i^{-\frac{\gamma}{2}}\mathbf{h}_i(m)\mathbf{B}_i(m)\times \\
&\quad \cos\left(\boldsymbol{\phi}_i(m)+\boldsymbol{\theta}_i(m)+\boldsymbol{\phi}_{\omega_m}\right)\mathbf{1}\left(\mathbf{L}_i\geq m-k+1>0\right)\Bigg)\Bigg\} \quad (5) \\
&= \exp\Bigg(\lambda\pi R^2\Bigg(-1+\mathbb{E}\Bigg\{\exp\Bigg(j\sum_{m=1}^{n}|\omega_m|\,\mathbf{r}^{-\frac{\gamma}{2}}\mathbf{h}(m)\mathbf{B}(m)\times \\
&\quad \cos\left(\boldsymbol{\phi}(m)+\boldsymbol{\theta}(m)+\boldsymbol{\phi}_{\omega_m}\right)\mathbf{1}\left(\mathbf{L}\geq m-k+1>0\right)\Bigg)\Bigg\}\Bigg)\Bigg) \quad (6)
\end{aligned}$$

where $|\omega_m| = \sqrt{\left(\omega_m^{(I)}\right)^2 + \left(\omega_m^{(Q)}\right)^2}$, $\phi_{\omega_m} = \tan^{-1}\left(\frac{\omega_m^{(Q)}}{\omega_m^{(I)}}\right)$, $\mathbf{1}(\cdot)$ is the indicator function, and the expectation in (6) is with respect to the set of random variables $\{\mathbf{r}, \mathbf{L}, \mathbf{h}(m), \mathbf{B}(m), \boldsymbol{\phi}(m), \boldsymbol{\theta}(m)\}$. Equation (5) holds since $\boldsymbol{\Xi}_{k,m} = \left\{\mathbf{R} : (\mathbf{R},\mathbf{L}) \in \boldsymbol{\Pi}^{(k)}, \mathbf{L} \geq m-k+1\right\}$ for $m \geq k$, and is an empty set for $m < k$. Equation (6) is derived using the probability generating functional (PGFL) of a homogeneous PPP [3] and holds since the node emissions, node lifetime, and fading are each assumed to be *i.i.d.* across time slots and nodes. Note that the expectation in (6) is conditioned such that the node locations are uniformly distributed over $b(0,R)$ [3], [10]. Using the identity

$$e^{ja\cos(\phi)} = \sum_{l=0}^{\infty} j^l \boldsymbol{\epsilon}_l J_l(a)\cos(l\phi) \quad (7)$$

where $\boldsymbol{\epsilon}_0 = 1$, $\boldsymbol{\epsilon}_l = 2$ for $l \geq 1$, and $J_l(\cdot)$ denotes the Bessel function of order l, the log-characteristic function $\psi_{\overline{\mathbf{I}}_{k,1:n}}(\overline{\omega}_{1:n}) \triangleq \log \Phi_{\overline{\mathbf{I}}_{k,1:n}}(\overline{\omega}_{1:n})$ can be expressed as

$$\begin{aligned}
&\psi_{\overline{\mathbf{I}}_{k,1:n}}(\overline{\omega}_{1:n}) \\
&=\lambda\pi R^2\Bigg[-1+\mathbb{E}\Bigg\{\prod_{m=1}^{n}\Bigg(\sum_{l=0}^{\infty} j^l\boldsymbol{\epsilon}_l J_l\Big(|\omega_m|\,\mathbf{r}^{-\frac{\gamma}{2}}\mathbf{h}(m)\mathbf{B}(m)\times \\
&\quad \mathbf{1}\left(\mathbf{L}\geq m-k+1>0\right)\Big)\cos\left(l\left(\boldsymbol{\phi}(m)+\boldsymbol{\theta}(m)+\boldsymbol{\phi}_{\omega_m}\right)\right)\Bigg)\Bigg\}\Bigg] \quad (8) \\
&=\lambda\pi R^2\Bigg[-1+\mathbb{E}\Bigg\{\prod_{m=1}^{n} J_0\Big(|\omega_m|\,\mathbf{r}^{-\frac{\gamma}{2}}\mathbf{h}(m)\mathbf{B}(m)\times \\
&\quad \mathbf{1}\left(\mathbf{L}\geq m-k+1>0\right)\Big)\Bigg\}\Bigg] \quad (9) \\
&=\lambda\pi R^2\Bigg[\sum_{s=1}^{n}\overline{F}_{\mathbf{L}}^{(k,n)}(s)\Bigg(-1+ \\
&\quad \mathbb{E}\Bigg\{\prod_{m=\max(1,k)}^{s} J_0\left(|\omega_m|\,\mathbf{r}^{-\frac{\gamma}{2}}\mathbf{h}(m)\mathbf{B}(m)\right)\Bigg\}\Bigg)\Bigg] \quad (10)
\end{aligned}$$

where

$$\overline{F}_{\mathbf{L}}^{(k,n)}(s) = \begin{cases} 0 & s < k, \\ \mathbb{P}(\mathbf{L} = s-k+1) & k \leq s < n, \\ \mathbb{P}(\mathbf{L} \geq s-k+1) & s = n. \end{cases} \quad (11)$$

The expectation in (8) is with respect to the set of random variables $\{\mathbf{r}, \mathbf{L}, \mathbf{h}(m), \mathbf{B}(m), \boldsymbol{\phi}(m), \boldsymbol{\theta}(m)\}$. Equation (9) involves expanding the expectation over $\boldsymbol{\phi}(m)$ and $\boldsymbol{\theta}(m)$, where $\boldsymbol{\phi}(m), \boldsymbol{\theta}(m)$ are mutually independent and uniformly distributed in $[0, 2\pi]$ and *i.i.d.* across time slots m, and noting that $\mathbb{E}_{\boldsymbol{\phi}(m),\boldsymbol{\theta}(m)}\{\cos(l(\boldsymbol{\phi}(m)+\boldsymbol{\theta}(m)+\phi_{\omega_m}))\} = 0$ for $l \geq 1$ for all time slots m. Equation (10) is derived by expanding the expectation over the lifetime random variable $\mathbf{L}$. The expectation in (10) is thus with respect to the set of random variables $\{\mathbf{r}, \mathbf{h}(m), \mathbf{B}(m)\}$. To further simplify (10), we express it as

$$\psi_{\overline{\mathbf{I}}_{k,1:n}}(\overline{\omega}_{1:n}) = \lambda\pi\left[\sum_{s=1}^{n}\overline{F}_{\mathbf{L}}^{(k,n)}(s)\Upsilon_{(k,s)}(\overline{\omega}_{1:n})\right] \quad (12)$$

where for any parameters $\{k, s\}$,

$$\begin{aligned}
&\Upsilon_{(k,s)}(\overline{\omega}_{1:n}) \\
&= \lim_{R\to\infty} R^2\Bigg(-1+ \\
&\quad \mathbb{E}\Bigg\{\prod_{m=\max(1,k)}^{s} J_0\left(|\omega_m|\,\mathbf{r}^{-\frac{\gamma}{2}}\mathbf{h}(m)\mathbf{B}(m)\right)\Bigg\}\Bigg) \quad (13) \\
&= \lim_{R\to\infty} R^2\Bigg(-1+ \\
&\quad \int_0^R \prod_{m=\max(1,k)}^{s}\mathbb{E}_{\mathbf{h},\mathbf{B}}\left\{J_0\left(|\omega_m|\,r^{-\frac{\gamma}{2}}\mathbf{h}\mathbf{B}\right)\right\}\frac{2r}{R^2}dr\Bigg) \quad (14) \\
&= -\int_0^{\infty}\frac{\partial}{\partial r}\left(\prod_{m=\max(1,k)}^{s}\mathbb{E}_{\mathbf{h},\mathbf{B}}\left\{J_0\left(|\omega_m|\,r^{-\frac{\gamma}{2}}\mathbf{h}\mathbf{B}\right)\right\}\right)r^2 dr. \quad (15)
\end{aligned}$$

Equation (14) is derived by expanding the expectation over $\mathbf{r}$ in (13) and noting that $\mathbf{h}(m)$ and $\mathbf{B}(m)$ are each *i.i.d.* across time slots m. Equation (15) involves integrating (14) by parts and using the series expansion of $J_0(x)$ around $x{=}0$ to show that $\lim_{R\to\infty} R^2\left(-1+\prod_{m=\max(1,k)}^{s}\mathbb{E}_{\mathbf{h},\mathbf{B}}\left\{J_0\left(|\omega_m|\,R^{-\frac{\gamma}{2}}\mathbf{h}\mathbf{B}\right)\right\}\right){=}0$ for $\gamma{>}2$.

Exact evaluation of (15) is possible for $s = \max(1,k)$, i.e., when only one $J_0(\cdot)$ term exists, which arises in deriving the instantaneous statistics of interference and reduces to an isotropic alpha stable form $\left(\propto |\omega_s|^{\frac{4}{\gamma}}\right)$ [10], [11]. Similar reduction with exact equality, however, is not possible for terms involving a product of Bessel functions. We thus propose an approximation of the log-characteristic function for $|\omega_m|, m = 1, \cdots, n$ in the neighborhood of zero based on an identity proposed by Middleton [17]. From Fourier analysis, the behavior of the characteristic function for $|\omega_m|, m = 1, \cdots, n$ in the neighborhood of zero governs the joint tail probability of the random envelope at time instants 1 through n. The proposed approximation is based on the following identity [17]:

$$\mathbb{E}_{\mathbf{h},\mathbf{B}}\left\{J_0\left(|\omega_m|\,r^{-\frac{\gamma}{2}}\mathbf{h}\mathbf{B}\right)\right\} = e^{-\frac{|\omega_m|^2 r^{-\gamma}\mathbb{E}_{\mathbf{h},\mathbf{B}}\left\{\mathbf{h}^2\mathbf{B}^2\right\}}{4}}\times (1+\boldsymbol{\Lambda}(|\omega_m|)) \quad (16)$$

where $\mathbf{\Lambda}(|\omega_m|)$ indicates a correction term with the lowest exponent in $|\omega_m|$ of four and is given by

$$\mathbf{\Lambda}(|\omega_m|) = \sum_{k=2}^{\infty} \frac{\left(\mathbb{E}_{\mathbf{Z}}\left\{\mathbf{Z}\right\}\right)^k |\omega_m|^{2k} r^{-k\gamma}}{2^{2k}k!} \times \mathbb{E}_{\mathbf{Z}}\left\{ {}_1F_1\left(-k;1;\frac{\mathbf{Z}}{\mathbb{E}_{\mathbf{Z}}\left\{\mathbf{Z}\right\}}\right)\right\} \quad (17)$$

where the random variable $\mathbf{Z} = \mathbf{h}^2\mathbf{B}^2$, and ${}_1F_1\left(a;b;x\right)$ is the confluent hypergeometric function of the first kind. Also $\mathbf{\Lambda}(|\omega_m|) = O\left(|\omega_m|^4\right)$ as $|\omega_m| \to 0$.

Using this identity, and approximating $\mathbf{\Lambda}(|\omega_m|) \ll 1$ for $|\omega_m|, m = 1, \cdots, n$ in the neighborhood of zero, (15) reduces to

$$\Upsilon_{(k,s)}\left(\overline{\omega}_{1:n}\right) \approx -\int_0^{\infty} \frac{\partial}{\partial r}\Big(e^{-\frac{\left(\sum_{m=\max(1,k)}^{s}|\omega_m|^2\right)r^{-\gamma}\mathbb{E}_{\mathbf{h},\mathbf{B}}\left\{\mathbf{h}^2\mathbf{B}^2\right\}}{4}}\Big) r^2 dr \quad (18)$$

$$= -\left[\left(\sum_{m=\max(1,k)}^{s}|\omega_m|^2\right)\frac{\mathbb{E}_{\mathbf{h},\mathbf{B}}\left\{\mathbf{h}^2\mathbf{B}^2\right\}}{4}\right]^{\frac{2}{\gamma}}\Gamma\left(1-\frac{2}{\gamma}\right) \quad (19)$$

where $\Gamma(\cdot)$ denotes the Gamma function. When $\mathbf{hB}$ is Rayleigh distributed, e.g., for constant amplitude modulated transmissions in Rayleigh fading environment, then $\mathbf{\Lambda}(|\omega_m|) = 0$ and the expression in (18) is exact. Substituting (19) in (12), the log-characteristic function can be expressed as

$$\psi_{\overline{\mathbf{I}}_{k,1:n}}(\overline{\omega}_{1:n}) = -\overline{\sigma}\left[\sum_{s=1}^{n}\overline{F}_{\mathbf{L}}^{(k,n)}(s)\left(\sqrt{\sum_{m=\max(1,k)}^{s}|\omega_m|^2}\right)^{\frac{4}{\gamma}}\right] \quad (20)$$

where $\overline{\sigma} = \lambda\pi\left(\frac{\mathbb{E}_{\mathbf{h},\mathbf{B}}\left\{\mathbf{h}^2\mathbf{B}^2\right\}}{4}\right)^{\frac{2}{\gamma}}\Gamma\left(1-\frac{2}{\gamma}\right)$ and $\overline{F}_{\mathbf{L}}^{(k,n)}(\cdot)$ is defined in (11). Equation (20) corresponds to a $2n$-dimensional symmetric alpha stable vector with characteristic exponent $\alpha = \frac{4}{\gamma}$ [18].

B. Network Model II

Let $\overline{\mathbf{I}}_{1:n} = \left\{\mathbf{I}_1^{(I)}, \mathbf{I}_1^{(Q)}, \mathbf{I}_2^{(I)}, \mathbf{I}_2^{(Q)}, \cdots, \mathbf{I}_n^{(I)}, \mathbf{I}_n^{(Q)}\right\}$ denote the vector of in-phase and quadrature phase components on the interference at time slots 1 through n due to nodes that emerged anytime till slot n. Using (3) and noting that the underlying Poisson process of emerging nodes at any time slots k are mutually independent for all k, the joint log-characteristic function of $\overline{\mathbf{I}}_{1:n}$ can be expressed as

$$\boldsymbol{\psi}_{\overline{\mathbf{I}}_{1:n}}\left(\overline{\omega}_{1:n}\right) = \sum_{k=-\infty}^{n}\boldsymbol{\psi}_{\overline{\mathbf{I}}_{k,1:n}}\left(\overline{\omega}_{1:n}\right). \quad (21)$$

Substituting (20) in (21), the log-characteristic function can be expanded as shown in (22), where $\overline{\sigma} = \lambda\pi\left(\frac{\mathbb{E}_{\mathbf{h},\mathbf{B}}\left\{\mathbf{h}^2\mathbf{B}^2\right\}}{4}\right)^{\frac{2}{\gamma}}\Gamma\left(1-\frac{2}{\gamma}\right)$. Equation (22) is the log-characteristic function of a $2n$-dimensional symmetric alpha stable vector with characteristic exponent $\alpha = \frac{4}{\gamma}$. Intuition into the above form of the log-characteristic function can be gained as follows. Each of the $\left(\sqrt{|\omega_i|^2 + \cdots + |\omega_j|^2}\right)^{\alpha}$ term in (22) contributes to the joint characteristic function at dimensions corresponding to the interference at time slots i through j. Further, the parameter λ embedded inside $\overline{\sigma}$, along with the probability on the random variable $\mathbf{L}$, forms a pre-multiplier to the terms $\left(\sqrt{|\omega_i|^2 + \cdots + |\omega_j|^2}\right)^{\alpha}$, and corresponds to the density of users that are active only during the time slots i through j. For example, the density of users affecting interference only at time slots 1 and 2 includes users that emerged at time slot $k \leq 1$ and are active until time slot 2, i.e., $\sum_{k\leq 1}\lambda\mathbb{P}(\mathbf{L} = 3-k) = \lambda\mathbb{P}(\mathbf{L} \geq 2)$. The user density $\lambda\mathbb{P}(\mathbf{L} \geq 2)$ thus forms a pre-multiplier for the term $\left(\sqrt{|\omega_1|^2 + |\omega_2|^2}\right)^{\alpha}$ in (22).

C. Joint Tail Probability of Interference Amplitude

We are interested in deriving closed-form expressions for the joint interference tails of the form

$$\mathbb{P}(\Delta > n) = \mathbb{P}\left(\|\mathbf{I}_1\| > \beta_1, \|\mathbf{I}_2\| > \beta_2, \cdots, \|\mathbf{I}_n\| > \beta_n\right) \quad (23)$$

where Δ is the number of consecutive failed transmissions. Recall that for analysis of network model I, $k = 1$ can be assumed without loss of generality. Hence, we use $\mathbf{I}_n$ to denote the interference at time slot n for both the network models. Further, for simplicity in exposition, we assume non-random thresholds β_i in this subsection. In the later sections, the tail thresholds β_i are inherently random as they relate to the random signal power. Since the interference and the desired signal are independent, the results derived in this subsection are used directly and averaged over the randomness in signal power.

For both the network models, the joint characteristic function of interference at time slots 1 through n was shown to follow a $2n$-dimensional symmetric alpha stable distribution. Even though we derived the joint characteristic function of interference in a known form, expressing the joint tail probability in closed-form turns out to be nontrivial. Referring to (20) and (22), the log-characteristic function is a sum of many $\left(\sqrt{\sum_m |\omega_m|^2}\right)^{\alpha}$ terms. To the best of our knowledge, no direct result is available in the literature to aid the derivation of (23) in closed-form for this specific form of joint characteristic function. To this end, we provide certain useful theorems regarding the tail probability of symmetric alpha stable vectors with the same mathematical form as (20) and (22).

We now briefly describe the steps required to derive the joint tail probability in closed-form using the results proved in Appendix A. Theorem A.2 is the key underlying theorem, and expresses the tail probability of the form (23) in terms of the symmetric alpha stable spectral measure in an integral form. The spectral measure, along with the characteristic exponent α, completely characterize the statistics of a symmetric alpha stable vector (see Theorem 2.4.3 in [18]). Further, for the log-characteristic function of the form (20) and (22), we observe

$$\boldsymbol{\psi}_{\overline{\mathbf{I}}_{1:n}}(\overline{\omega}_{1:n}) = -\overline{\sigma}\Bigg[\mathbb{P}(\mathbf{L}\geq 1)\left(\left(\sqrt{|\omega_1|^2}\right)^{\alpha}+\left(\sqrt{|\omega_n|^2}\right)^{\alpha}\right)+\mathbb{P}(\mathbf{L}=1)\left(\sum_{l=2}^{n-1}\left(\sqrt{|\omega_l|^2}\right)^{\alpha}\right)+$$
$$\mathbb{P}(\mathbf{L}\geq 2)\left(\left(\sqrt{|\omega_1|^2+|\omega_2|^2}\right)^{\alpha}+\left(\sqrt{|\omega_{n-1}|^2+|\omega_n|^2}\right)^{\alpha}\right)+\mathbb{P}(\mathbf{L}=2)\left(\sum_{l=2}^{n-2}\left(\sqrt{|\omega_l|^2+|\omega_{l+1}|^2}\right)^{\alpha}\right)+$$
$$\vdots$$
$$\mathbb{P}(\mathbf{L}\geq n-1)\left(\left(\sqrt{|\omega_1|^2+|\omega_2|^2+\cdots+|\omega_{n-1}|^2}\right)^{\alpha}+\left(\sqrt{|\omega_2|^2+|\omega_3|^2+\cdots+|\omega_n|^2}\right)^{\alpha}\right)+$$
$$(\mathbb{P}(\mathbf{L}\geq n)+\mathbb{P}(\mathbf{L}\geq n+1)+\cdots)\left(\sqrt{|\omega_1|^2+|\omega_2|^2+\cdots+|\omega_n|^2}\right)^{\alpha}\Bigg] \quad (22)$$

that the spectral measure $\overline{\Gamma}$ on the $2n$-dimensional unit sphere S_{2n} can be represented as a sum of independent measures

$$\overline{\Gamma} = \overline{\Gamma}_0 + \sum_{k=1}^{|\mathcal{X}|}\overline{\Gamma}_k\delta\left(\bigcup_{j\in\mathcal{X}(k)}\{s_{2j-1},s_{2j}\}\right), \quad (24)$$

where $\mathcal{X}$ is a collection of non-empty proper subsets of $\{1,2,\cdots,n\}$, $|\mathcal{X}|$ denotes the cardinality of $\mathcal{X}$, $\mathcal{X}(k)$ is the k^{th} set contained in $\mathcal{X}$, $\delta(\cdots)$ denotes the multi-dimensional dirac delta functional, $s\in S_{2n}$, $\overline{\Gamma}_0$ is a spectral measure distributed over the unit sphere S_{2n}, and $\overline{\Gamma}_k$ is a spectral measure distributed over the unit sphere $S_{2(n-|\mathcal{X}(k)|)}$ formed from the dimensions $\cup_{j=1,\cdots,2n;j\notin\mathcal{X}(k)}\{2j-1,2j\}$.

For symmetric alpha stable vectors with a spectral measure of the form (24), we prove in Corollary A.2.1 that the joint tail probability of the form (23) is dominated by the measure $\overline{\Gamma}_0$. In other words, the joint tails are dominated by the $\left(\sqrt{|\omega_1|^2+\cdots+|\omega_n|^2}\right)^{\alpha}$ term in the log-characteristic function when $\beta_1,\cdots,\beta_n\to\infty$ with the same rate. Further, since the spectral measure $\overline{\Gamma}_0$ is uniformly distributed over the unit sphere S_{2n}, it implies that the tails are equivalent to the tails of an isotropic symmetric alpha stable vector with a spectral measure $\overline{\Gamma}_0$ [18]. For an isotropic symmetric alpha stable vector, we have derived the tail probability in closed-form in Theorem A.1.

Using the aforementioned proof outline, if $\beta_i=\beta\eta_i$ for $0<\eta_i<\infty$, then

$$\lim_{\beta\to\infty}\left(\sqrt{\sum_{i=1}^{n}\beta_i^2}\right)^{\alpha}\mathbb{P}(\Delta>n) = 2^{\alpha}\overline{\sigma}\mathcal{F}_{\mathbf{L}}(n)C_{\frac{\alpha}{2}}\cos\left(\frac{\pi\alpha}{4}\right)\Gamma\left(1+\frac{\alpha}{2}\right) \quad (25)$$

where

$$\mathcal{F}_{\mathbf{L}}(n) = \begin{cases}\mathbb{P}(\mathbf{L}\geq n) & \text{for network model I,}\\ \sum_{k=n}^{\infty}\mathbb{P}(\mathbf{L}\geq k) & \text{for network model II,}\end{cases} \quad (26)$$

and $C_{\frac{\alpha}{2}}$ is given by (46). Equation (25) is derived using Corollary A.2.1, recognizing that $\overline{\Gamma}_0$ is uniformly distributed over S_{2n}, and finally using Theorem A.1. Thus for $\beta_1,\cdots,\beta_n$ large,

$$\mathbb{P}(\Delta>n) \approx \left(\sqrt{\sum_{i=1}^{n}\beta_i^2}\right)^{-\alpha} 2^{\alpha}\overline{\sigma}\mathcal{F}_{\mathbf{L}}(n)C_{\frac{\alpha}{2}}\cos\left(\frac{\pi\alpha}{4}\right)\Gamma\left(1+\frac{\alpha}{2}\right). \quad (27)$$

Intuitively, the joint tail probability is dominated by the $\left(\sqrt{|\omega_1|^2+\cdots+|\omega_n|^2}\right)^{\alpha}$ term in the log-characteristic function since this term corresponds to the contribution by nodes that are active at all time slots 1 through n. The event that the interference amplitude is high at all time slots 1 though n is more likely to be due to the nodes that were active at all time slots, rather than due to nodes that were active in only some of those time slots.

IV. Single Hop Communication Performance Analysis

In this section, we use the joint tail probability of interference to derive the descriptive measures of communication performance for single hop transmissions. For both network models, we assume the network is interference limited and so thermal noise can be ignored.

A. Local Delay

Local delay (LD) of the network is defined as the expected number of time slots a typical node requires for a successful transmission to its receiver. In other words, the local delay is one more than the expected number of successive failed transmission attempts ($\mathbb{E}\{\Delta\}$) of a typical node. Since a node is active for a maximum of L_{max} time slots, the local delay of the network can be expressed as

$$\mathtt{LD}=1+\mathbb{E}\{\Delta\}$$
$$=1+\sum_{n=1}^{L_{max}}\mathbb{P}(\mathtt{SIR}_1<T,\mathtt{SIR}_2<T,\cdots,\mathtt{SIR}_n<T) \quad (28)$$
$$=1+\sum_{n=1}^{L_{max}}\mathbb{P}(\|\mathbf{I}_1\|>\beta_1,\|\mathbf{I}_2\|>\beta_2,\cdots,\|\mathbf{I}_n\|>\beta_n) \quad (29)$$

where $\beta_n^2=T^{-1}D^{-\gamma}\mathbf{h}_0^2(n)\mathbf{B}_0^2(n)$, and T is the SIR threshold required for successful detection. Thus the local delay can be expressed as the joint tail probability of interference.

To enforce a low outage regime, we assume $T \ll 1$. The assumption $T \ll 1$ is particularly valid for spread spectrum physical layer where T^{-1} is proportional to the spreading gain. While the results are asymptotically exact for $T \ll 1$, simulations show that they match closely for typical values of T around -5dB to -10dB. For $T \ll 1$, β_n is large and thus by using (27) we have

$$\texttt{LD} \approx 1 + T^{\frac{\alpha}{2}} D^2 \lambda K(\alpha) \left(\mathbb{E}\left\{\mathbf{h}^2\mathbf{B}^2\right\}\right)^{\frac{\alpha}{2}} \times \sum_{n=1}^{L_{max}} \left[\mathbb{E}\left\{\left(\sum_{k=1}^{n} \mathbf{h}_0^2(k)\mathbf{B}_0^2(k)\right)^{-\frac{\alpha}{2}}\right\} \mathcal{F}_{\mathbf{L}}(n)\right] \quad (30)$$

where

$$K(\alpha) = \pi C_{\frac{\alpha}{2}} \cos\left(\frac{\pi\alpha}{4}\right) \Gamma\left(1 - \frac{\alpha}{2}\right) \Gamma\left(1 + \frac{\alpha}{2}\right). \quad (31)$$

Equation (30) expresses the local delay for network models I and II in closed-form. We can now observe the impact of various system parameters on the local delay.

User density: The intensity (λ) of the PPP has a linear effect on the local delay of the network.

Power pathloss exponent: Recall that the power pathloss exponent (γ) is related to the characteristic exponent as $\alpha = \frac{4}{\gamma}$. To gain insight into the effect of α on the local delay, we consider $\mathbb{E}(\Delta)$ for a non-random fading $(\mathbf{h}, \mathbf{h}_0(k))$ and non-random emission amplitudes $(\mathbf{B}, \mathbf{B}_0(k))$. The RHS of (30) becomes $T^{\frac{\alpha}{2}} D^2 \lambda K(\alpha) \sum_{n=1}^{L_{max}} n^{-\frac{\alpha}{2}} \mathcal{F}_{\mathbf{L}}(n)$. The factor $K(\alpha)$ does not vary significantly over a meaningful range of pathloss exponent ($2 < \gamma \leq 8$). Since this paper considers $T \ll 1$, increasing γ (or equivalently decreasing α) increases the local delay $\mathbb{E}(\Delta)$ exponentially. Intuitively, this happens because an interferer close to the desired receiver becomes even more dominant as compared to the desired signal if γ is large.

SIR threshold: Since $\alpha < 2$, local delay scales sublinearly ($T^{\frac{\alpha}{2}}$) with the SIR threshold (T).

Fading: To study the effect of fading, consider non-random emission amplitudes $(\mathbf{B}, \mathbf{B}_0(k))$. Evaluating (30) for Rayleigh fading with parameter $1/\sqrt{2}$ (i.e. , $\mathbf{h}_0^2(k) \sim \exp(1)$) gives

$$\texttt{LD} = 1 + T^{\frac{\alpha}{2}} D^2 \lambda K(\alpha) \sum_{n=1}^{L_{max}} \frac{\Gamma\left(n - \frac{\alpha}{2}\right)}{(n-1)!} \mathcal{F}_{\mathbf{L}}(n) \quad (32)$$

where the factor $\frac{\Gamma\left(n-\frac{\alpha}{2}\right)}{(n-1)!}$ is approximately equal to $n^{-\frac{\alpha}{2}}$. Further, for any fading and interferer emission distributions, local delay can be lower bounded by using the Jensen's inequality and recalling that $\mathbf{h}_0^2(k)\mathbf{B}_0^2(k)$ are mutually *i.i.d.* for all k, given as

$$\texttt{LD} \geq 1 + T^{\frac{\alpha}{2}} D^2 \lambda K(\alpha) \frac{\left(\mathbb{E}\left\{\mathbf{h}^2\mathbf{B}^2\right\}\right)^{\frac{\alpha}{2}}}{\mathbb{E}\left\{\mathbf{h}_0^{\alpha}\mathbf{B}_0^{\alpha}\right\}} \sum_{n=1}^{L_{max}} n^{-\frac{\alpha}{2}} \mathcal{F}_{\mathbf{L}}(n). \quad (33)$$

Equality in (33) is attained, for example, when $\mathbf{h}_0^2(k)\mathbf{B}_0^2(k)$ does not vary with k. Such a situation can occur when the desired node employs channel inversion power control by adapting its instantaneous transmission power $\mathbf{B}_0^2(k)$ to combat the variations due to channel fading $\mathbf{h}_0^2(k)$. Using (33), we can conclude that channel inversion power control reduces the local delay of the network.

Lifetime probability: From (30) we can conclude that the local delay increases as $\mathbb{E}(\mathbf{L})$ increases. This is also intuitively clear as increasing the mean lifetime of nodes causes more interference in the network. Further the static and highly mobile networks studied in prior work [5], [6] can be analyzed as particular cases of the network models I and II.

(a) Network model I with $\mathbf{L} \xrightarrow{p} \infty$: This would represent a static network with no node mobility, where given a particular instantiation of the PPP, the node actively transmit for a large number of time slots. Here $L_{max} \to \infty$, $\mathcal{F}_{\mathbf{L}}(n) = 1 \ \forall n$ from (26). Thus the local delay is

$$\texttt{LD} \geq 1 + T^{\frac{\alpha}{2}} D^2 \lambda K(\alpha) \sum_{n=1}^{\infty} n^{-\frac{\alpha}{2}} \to \infty \quad (34)$$

since $\alpha < 2$. This is the same result as [5], [6] for the Poisson bipolar model with no mobility, and a medium access probability of 1 in the slotted-ALOHA MAC protocol.

(b) Network model II with $\mathbf{L} \stackrel{p}{=} 1$: This would represent a highly mobile network, where the location of active nodes at each time slot is an independent instantiation of the PPP. Here $L_{max} = 1$, $\mathcal{F}_{\mathbf{L}}(1) = 1$, and $\mathcal{F}_{\mathbf{L}}(n) = 0$ for $n \geq 2$ from (26). The local delay for such a network is

$$\begin{aligned}\texttt{LD} &= 1 + T^{\frac{\alpha}{2}} D^2 \lambda K(\alpha) \frac{\left(\mathbb{E}\left\{\mathbf{h}^2\mathbf{B}^2\right\}\right)^{\frac{\alpha}{2}}}{\mathbb{E}\left\{\mathbf{h}_0^{\alpha}\mathbf{B}_0^{\alpha}\right\}} \\ &\geq 1 + T^{\frac{\alpha}{2}} D^2 \lambda K(\alpha) \end{aligned} \quad (35)$$

which is asymptotically ($T \ll 1$) same as the result in [5] for the Poisson bipolar model with high mobility, Rayleigh fading, and a medium access probability of 1 in the slotted-ALOHA MAC protocol.

B. Outage with respect to Throughput

Let $\mathbf{S}(n)$ denote the number of successful transmissions in n consecutive time slots. Then the outage probability associated with achieving at least s successful transmissions in n time slots is

$$\begin{aligned}&\mathbb{P}\left(\mathbf{S}(n) < s\right) \\ &= \mathbb{P}\left(\bigcup_{1 \leq i_1 \leq \cdots \leq i_{n-s+1} \leq n} \texttt{SIR}_{i_1} < T, \cdots, \texttt{SIR}_{i_{n-s+1}} < T\right) \\ &= \sum_{k=n-s+1}^{n} \left[(-1)^{k-(n-s+1)} \binom{k-1}{n-s} \times \right. \\ &\qquad \left. \sum_{1 \leq i_1 \leq \cdots \leq i_k \leq n} \mathbb{P}\left(\|\mathbf{I}_{i_1}\| > \beta_{i_1}, \cdots, \|\mathbf{I}_{i_k}\| > \beta_{i_k}\right)\right] \end{aligned} \quad (36)$$

for $1 \leq s \leq n$, where $\beta_i = \beta\eta_i$, $\beta^2 = T^{-1}D^{-\gamma}$, and $\eta_i^2 = \mathbf{h}_0^2(i)\mathbf{B}_0^2(i)$. Now for $I = \{i_1, \cdots, i_k\}$,

$$\begin{aligned}&\lim_{\beta \to \infty} \left(\sqrt{\sum_{l \in I} \beta_l^2}\right)^{\alpha} \mathbb{P}\left(\|\mathbf{I}_{i_1}\| > \beta_{i_1}, \cdots, \|\mathbf{I}_{i_k}\| > \beta_{i_k}\right) \\ &\qquad = 2^{\alpha} \overline{\sigma} \mathcal{M}_{\mathbf{L}}(i_1, i_k) C_{\frac{\alpha}{2}} \cos\left(\frac{\pi\alpha}{4}\right) \Gamma\left(1 + \frac{\alpha}{2}\right) \end{aligned} \quad (37)$$

where

$$\mathcal{M}_{\mathbf{L}}(i,j)=\begin{cases}\mathcal{F}_{\mathbf{L}}(j) & \text{for network model I,}\\ \mathcal{F}_{\mathbf{L}}(j-i+1) & \text{for network model II}\end{cases} \quad (38)$$

can be derived using (27) and noting that the log-characteristic function for $\left\{\mathbf{I}_{i_1}^{(I)},\mathbf{I}_{i_1}^{(Q)}\cdots,\mathbf{I}_{i_k}^{(I)},\mathbf{I}_{i_k}^{(Q)}\right\}$ is of the form (20) or (22) for network models I and II, respectively, with $|\omega_m|$ set to zero for $m\notin I$. Using (36) and (37), for β large we have

$$\begin{aligned}&\mathbb{P}\left(\mathbf{S}(n)<s\right)\\ &\approx\mathcal{K}\sum_{k=n-s+1}^{n}\Bigg[(-1)^{k-(n-s+1)}\binom{k-1}{n-s}\times\\ &\quad\sum_{1\le i_1\le\cdots\le i_k\le n}\mathbb{E}\left\{\left(\sum_{l\in I}\mathbf{h}_0^2(l)\mathbf{B}_0^2(l)\right)^{-\frac{\alpha}{2}}\right\}\mathcal{M}_{\mathbf{L}}(i_1,i_k)\Bigg]\\ &=\mathcal{K}\sum_{k=n-s+1}^{n}\Bigg[(-1)^{k-(n-s+1)}\binom{k-1}{n-s}\times\\ &\quad\mathbb{E}\left\{\left(\sum_{l=1}^{k}\mathbf{h}_0^2(l)\mathbf{B}_0^2(l)\right)^{-\frac{\alpha}{2}}\right\}\sum_{d=k}^{n}\mathcal{N}(n,k,d)\mathcal{F}_{\mathbf{L}}(d)\Bigg] \quad (39)\end{aligned}$$

where $\mathcal{K}=T^{\frac{\alpha}{2}}D^2\lambda K(\alpha)\left(\mathbb{E}\left\{\mathbf{h}^2\mathbf{B}^2\right\}\right)^{\frac{\alpha}{2}}$ and

$$\begin{aligned}&\mathcal{N}(n,k,d)\\ &=\begin{cases}\begin{cases}n & \text{for } k{=}1,\\ (n{-}d{+}1)\binom{d-2}{k-2} & \text{for } k{\ge}2,\end{cases} & \text{for network model I,}\\ \binom{d-1}{k-1} & \text{for network model II.}\end{cases}\end{aligned} \quad (40)$$

Trends similar to the local delay can be observed for $\mathbb{P}\left(\mathbf{S}(n)<s\right)$ as a function of various network parameters. Further, if a node is active for n consecutive time slots, the expected number of successes during those n time slots are $\mathbb{E}\left\{\mathbf{S}(n)\right\}=n-\sum_{s=1}^{n}\mathbb{P}\left(\mathbf{S}(n)<s\right)$.

C. Average Network Throughput (Network Model II)

We focus on network model II since the point process of active nodes is statistically invariant across time slots in this case. Recall that the spatial density of active nodes at any time slot is $\lambda\mathbb{E}\{\mathbf{L}\}$. Now consider a typical node in the network that is active for l consecutive time slots with probability $\mathbb{P}(\mathbf{L}=l)$. Assume that for each successful transmission, the typical node is able to communicate at $\log_2(1{+}T)$ bits/Hz, i.e., the Shannon rate. In l time slots, the typical node is expected to have $\mathbb{E}\left\{\mathbf{S}(l)\right\}$ successful transmissions, or an expected successful transmission rate of $\frac{\mathbb{E}\{\mathbf{S}(l)\}}{l}\log_2(1+T)$ bps/Hz. Averaging this rate over the lifetime distribution of a typical node, the average network throughput (in bps/Hz/area) is

$$\mathtt{C}^{\mathtt{av}}=\lambda\mathbb{E}\{\mathbf{L}\}\log_2(1+T)\mathbb{E}_{\mathbf{L}}\left\{\frac{\mathbb{E}\left\{\mathbf{S}(\mathbf{L})\right\}}{\mathbf{L}}\right\} \quad (41)$$

D. Transmission Capacity and Throughput-Delay-Reliability (TDR) Tradeoff (Network Model II)

The average throughput of the network discussed in the last subsection does not capture the quality-of-service constraints which may be required in most networks. Motivated by the approach used in [19], [20], we define the transmission capacity of the network and show that it captures the TDR tradeoff.

For single hop transmissions, delay can be interpreted as the number of time slots a typical node has to be active to achieve a desired throughput with a certain reliability. Thus $\mathbb{E}\{\mathbf{L}\}$ is considered to be the delay for single hop transmissions. This definition also enables us to study the TDR tradeoff of the network for different probability mass functions of the time slots that a node is active, $p_{\mathbf{L}}(l)$ for $l\in\{1,\cdots,L_{max}\}$, given a delay constraint $\mathbb{E}\{\mathbf{L}\}=\overline{L}$. Further, given an outage constraint of ϵ, we define

$$s^*(l,\epsilon)=\max\left\{s:\mathbb{P}\left(\mathbf{S}(l)<s\right)\le\epsilon\right\} \quad (42)$$

as the maximum number of successful transmissions in l time slots that can be achieved with reliability $(1-\epsilon)$. Hence a successful transmission rate of $\mathbb{E}_{\mathbf{L}}\left\{\frac{\mathbf{s}^*(\mathbf{L},\epsilon)}{\mathbf{L}}\right\}\log_2(1+T)$ bps/Hz can be achieved with reliability of $(1-\epsilon)$ for each user. We define the transmission capacity of the network (in bps/Hz/area) as

$$\begin{aligned}\mathtt{TC}(\overline{L},\epsilon)\triangleq\max_{\substack{p_{\mathbf{L}}(l),l\in\{1,\cdots,L_{max}\},\\ \mathbb{E}\{\mathbf{L}\}=\overline{L}}}\Bigg(&\lambda\overline{L}\log_2(1{+}T){\times}\\ &\mathbb{E}_{\mathbf{L}}\left\{\frac{s^*(\mathbf{L},\epsilon)}{\mathbf{L}}\right\}(1{-}\epsilon)\Bigg).\end{aligned} \quad (43)$$

Thus transmission capacity captures the TDR tradeoff, where the successful throughput of $\mathtt{TC}(\overline{L},\epsilon)$ bps/Hz/area can be achieved under a reliability constraint of $(1-\epsilon)$ and delay constraint $\mathbb{E}\{\mathbf{L}\}=\overline{L}$. For a given $(\overline{L},\epsilon)$ pair, $\mathtt{TC}(\overline{L},\epsilon)$ can be evaluated using numerical optimization of (43) over feasible lifetime distributions. Further, for a given distribution of $\mathbf{L}$, closed-form expression for $\mathbb{P}\left(\mathbf{S}(n)<s\right)$ in (39) enables direct numerical evaluation of (43), without requiring any Monte Carlo simulations of the network.

V. Simulation Results

Using the physical model discussed in Section I-B, we apply Monte Carlo numerical techniques to simulate the dynamics of network models I and II. A typical link is simulated by generating the desired transmission link in the presence of network interference using (1) and (3) for network models I and II, respectively. The empirical performance measures are then compared against the closed-form expressions for the corresponding measures derived in this paper. Even though the paper assumes that T^{-1} is large for deriving closed-form expressions, simulations reveal that the results match closely for considerably small values of T^{-1} of around $5-10$.

Unless mentioned otherwise, the network model parameters used in numerical simulations are:

$$\gamma=4,\lambda=0.01,\mathbf{h}\sim\text{Rayleigh}\left(1/\sqrt{2}\right),\mathbf{B}=5,$$

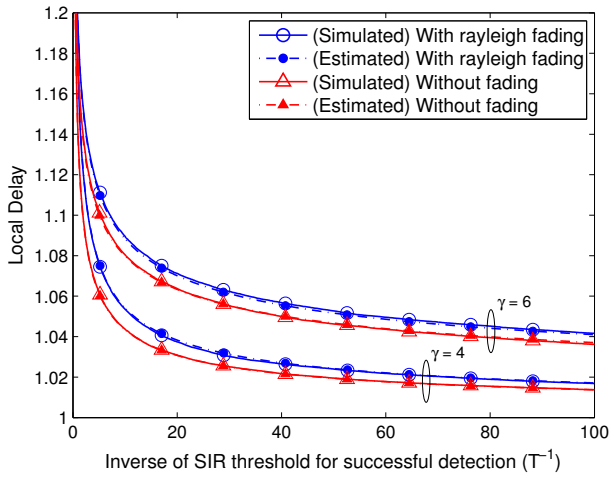

Fig. 3: Local delay in network model I with and without power control, $L_{max} = 20$ ($\overline{L} = 10$), and power pathloss exponent γ of $\{4, 6\}$. Local delay increases sublinearly as SIR threshold T required for successful detection increases, and exponentially as the power pathloss exponent increases. Channel inversion power control reduces the local delay of the network.

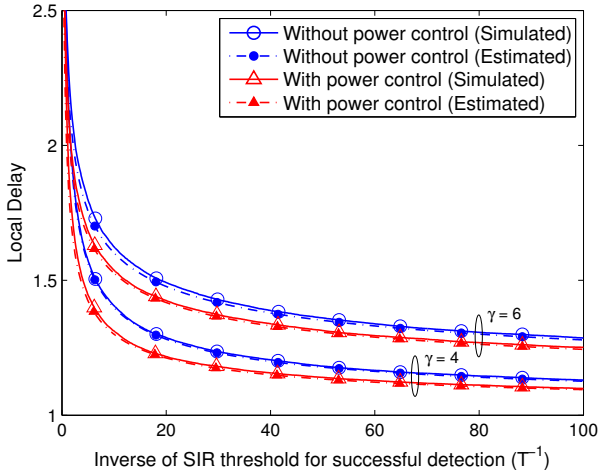

Fig. 4: Local delay in network model II with and without power control, $L_{max} = 20$ ($\overline{L} = 10$), and power pathloss exponent γ of $\{4, 6\}$. Variations of local delay with various network parameters are similar to those observed for network model I in Fig. 3.

and the lifetime ($\mathbf{L}$) of a typical node is assumed to follow a truncated Poisson distribution given as

$$\mathbf{L} \sim \left(\sum_{l=1}^{L_{max}} \frac{\overline{L}^l}{l!} \right)^{-1} \frac{\overline{L}^l}{l!} \qquad l = 1, \cdots, L_{max}, \tag{44}$$

where L_{max} and $\overline{L}$ are the maximum and the average number of time slots a node is active, respectively. In our simulations $\overline{L}$ is chosen to be $\frac{L_{max}}{2}$.

Local Delay: Figs. 3 and 4 compare the empirical and estimated local delay for network models I and II, respectively, as a function of the inverse of the SIR threshold $\left(T^{-1}\right)$ required for successful detection. Transmit power control is implemented by adapting the instantaneous transmission power $\mathbf{B}_0^2(k)$ to the channel fading conditions $\mathbf{h}_0^2(k)$ over time slots k, such that $\mathbf{h}_0^2(k)\mathbf{B}_0^2(k) = \mathbf{B}^2 = 25$.

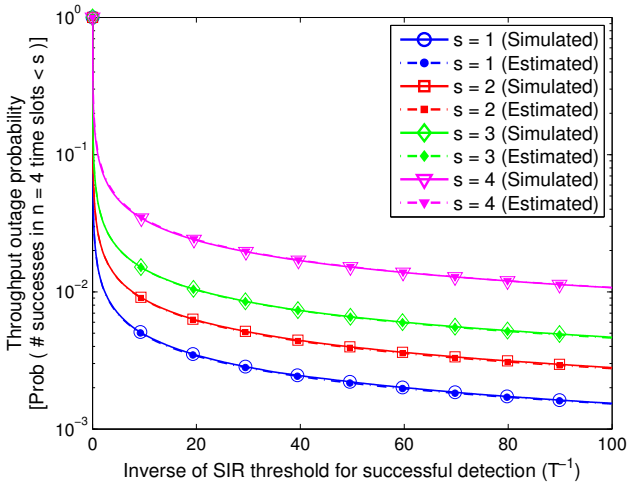

Fig. 5: Outage probability associated with achieving at least $s = \{1, 2, 3, 4\}$ successes in $n = 4$ time slots for network model I with $L_{max} = 20$.

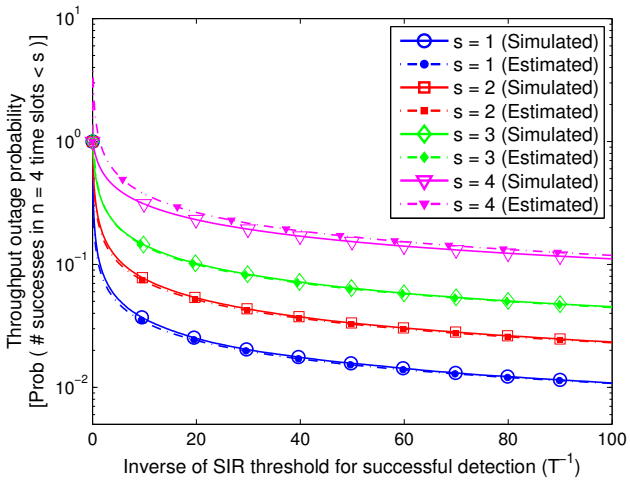

Fig. 6: Outage probability associated with achieving at least $s = \{1, 2, 3, 4\}$ successes in $n = 4$ time slots for network model II with $L_{max} = 20$.

Outage with respect to Throughput: Figs. 5 and 6 compare the empirical and estimated throughput outage probability for network models I and II, respectively, as a function of the inverse of the SIR threshold T^{-1}. Note that $\mathbb{P}(\mathbf{S}(n = 4) < 1)$ ($s = 1$ in Figs. 5 and 6) corresponds to the probability of outage in all $n = 4$ time slots. Hence Figs. 5 and 6 also serve as a verification of the result on joint tail probability of interference derived in (27). Additionally, for network model II, Fig. 7 compares the throughput outage probability when the channel coherence time is much larger than the symbol time period ($\mathtt{T_{coh}} = 10 \times \mathtt{T_{sym}}$). Though the paper assumes temporally *i.i.d.* channel $\mathbf{h}(\cdot)$ to derive the closed-form results, Fig. 7 shows that the large scale trends (i.e., decay rate of $\mathbb{P}(\mathbf{S}(n) < s)$) correspond closely in simulations even for slow fading channels. Similar correspondence in large scale trends for slow fading channels is observed for other communication performance measures derived in this paper.

Average Network Throughput (Network Model II): Fig. 8 compares the simulated and estimated average network

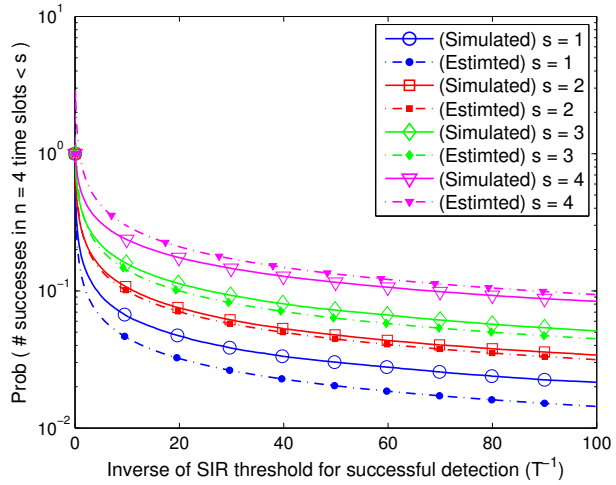

Fig. 7: Outage probability associated with achieving at least $s = \{1, 2, 3, 4\}$ successes in $n = 4$ time slots for network model II with $L_{max} = 20$ and $\mathtt{T_{coh}} = 10 \times \mathtt{T_{sym}}$, where $\mathtt{T_{coh}}$ and $\mathtt{T_{sym}}$ denotes the channel coherence time and symbol time period, respectively. Although the throughput outage probability is derived assuming fast fading (i.e., $\mathtt{T_{coh}} < \mathtt{T_{sym}}$), the decay rate of the outage probability matches closely to the simulated results even with slow fading.

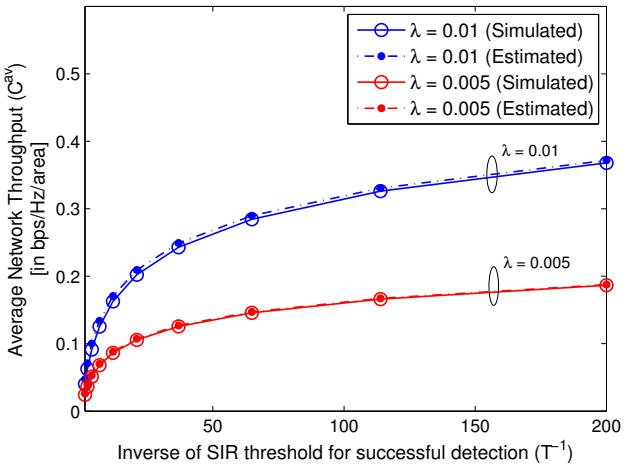

Fig. 8: Average throughput for network model II for $L_{max} = 10$, $\overline{L} = 5$, and $\lambda = \{0.01, 0.005\}$.

throughput as a function of T^{-1} for $\lambda = \{0.01, 0.005\}$. Increasing λ results in a increased spatial density of transmissions, but also increases interference at any receiver. Thus the average throughput grows sublinearly with λ.

Transmission Capacity and Throughput-Delay-Reliability (TDR) Tradeoff (Network Model II): Fig. 9 compares the transmission capacity as a function of the outage constraint ϵ. The optimization problem in (43) is solved numerically using the `fmincon` function in `MATLAB` using the active-set algorithm [21]. When higher outages are tolerable, increasing $\overline{L}$ increases the transmission capacity of the network since the spatial density of users transmitting at any time slot ($= \lambda\overline{L}$) increases more than the loss suffered due to increased interference. When outages are constrained to be low ($\epsilon < 0.1$ in Fig. 9), increasing $\overline{L}$ decreases the transmission capacity as interference becomes

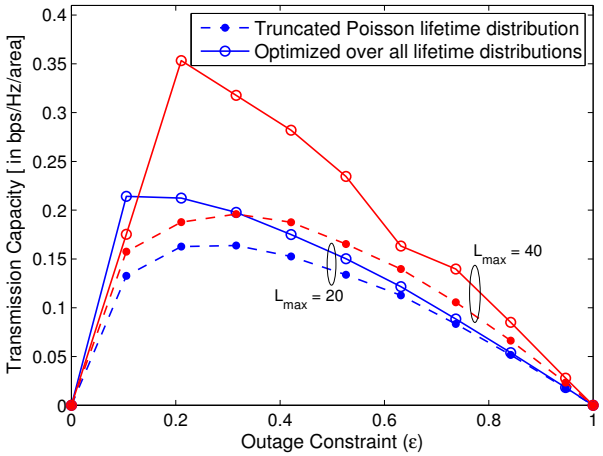

Fig. 9: Transmission capacity $\mathtt{TC}(\overline{L}, \epsilon)$ of network model II as a function of the outage constraint ϵ and delay constraint of $\overline{L} = \frac{L_{max}}{2} = \{20, 10\}$ for a `SIR` detection threshold T of 0.1. Transmission capacity with a truncated Poisson lifetime distribution is compared with that obtained by numerical optimization over feasible lifetime distributions. Optimizing over feasible lifetime distributions improves the peak throughput, and the reliability at which the peak throughput is achieved.

a limiting factor. Further, optimizing over all feasible lifetime distributions not only increases the peak throughput, but also improves the reliability at which the peak throughput is achieved. This motivates the design of MAC strategies that achieve the optimal lifetime distribution.

From a practical viewpoint, the simulations results provide the following insights. For a packet length of PL symbols, instead of transmitting $\overline{\mathbf{L}}$/PL packets for each channel access grant, the network interference is better managed by randomly varying the packet count. The optimal packet count distribution (lifetime distribution) is obtained by solving (43). Fig. 9 demonstrates up to $2\times$ in the peak network throughput, and a reliability improvement from approximately 0.8 to 0.9 (i.e., 50% fewer packet retransmissions) by optimizing the lifetime distribution. The gains in throughput and reliability are greater if more randomness in the packet count can be observed (i.e., greater L_{max}). Further, Figs. 3 through 8 show that reducing the detection threshold (via coding or other physical methods) significantly improves the delay and outage performance. This motivates design of physical layer methods to improve the detection performance in view of the non-Gaussian statistics of interference.

VI. Conclusions

The paper utilized the approximate temporal statistics of interference amplitude to derive network performance measures in simple algebraic form. This approach deviates from the mathematical techniques commonly used in literature for analyzing various network performance measures. While not shown in the paper, using such common methods to derive measures such as local delay for the network model assumed in this paper yields rather intractable results, thereby providing minimal insight into the effect of various network parameters on the communication performance. The non-Gaussian statistics of interference derived in this paper can be used to design

physical layer methods, such as filtering, detection rules, and forward error correcting codes, to improve the link spectral efficiency by several bps/Hz [22]–[24].

The results derived in this paper can be easily extended to include a slotted-ALOHA channel access protocol [25] in conjunction with the network model assumed in the paper. The analytical form of the results remain the same, with $\mathcal{F}_{\mathbf{L}}(n)$ replaced with $p^n\mathcal{F}_{\mathbf{L}}(n)$, where p is the channel access probability. Further, for a bounded pathloss function $\min(1, r^{-\frac{\gamma}{2}})$, the interference statistics can be derived using similar steps used in this paper and shown to follow a multivariate Gaussian mixture distribution [10]. The approach used in this paper can also be extended for frequency selective channels. Extensions to networks with contention based MAC protocols, however, appear nontrivial, but approximations may be proposed based on a Poisson assumption with a guard zone, which results in multivariate Gaussian mixture distributed interference [10], [26].

Appendix A
Statistical Properties of Symmetric Alpha Stable Random Vectors

This appendix borrows heavily from the notation, theorems, and proofs used in [18], while still being consistent with the notation used in this paper. We first derive the following theorem regarding the joint amplitude tails of an *isotropic* symmetric alpha stable vector.

Theorem A.1. *Let $\mathbf{X} = (\mathbf{X}_{1,I}, \mathbf{X}_{1,Q}, \cdots, \mathbf{X}_{d,I}, \mathbf{X}_{d,Q})$ be an isotropic symmetric alpha stable vector in $\mathbb{R}^{2d}$ with $0 < \alpha < 2$ and dispersion parameter σ [18]. Then the joint tail probability of $\|\mathbf{X}_1\|, \cdots, \|\mathbf{X}_d\|$ can be expressed as*

$$\lim_{\beta\to\infty} \beta^{\alpha}\mathbf{P}\left(\|\mathbf{X}_1\| > \beta_1, \cdots, \|\mathbf{X}_d\| > \beta_d\right) = 2^{\alpha}\sigma C_{\frac{\alpha}{2}} \cos\left(\frac{\pi\alpha}{4}\right)\Gamma\left(1+\frac{\alpha}{2}\right) \quad (45)$$

where $\beta = \sqrt{\sum_{i=1}^{d}\beta_i^2}$, $\|\mathbf{X}_i\| = \sqrt{\mathbf{X}_{i,I}^2 + \mathbf{X}_{i,Q}^2}$, and

$$C_{\alpha} = \begin{cases} \frac{2}{\pi} & \text{when } \alpha = 1, \\ \frac{1-\alpha}{\Gamma(2-\alpha)\cos\left(\frac{\pi\alpha}{2}\right)} & \text{otherwise}. \end{cases} \quad (46)$$

Proof: Using the sub-Gaussian representation of an isotropic symmetric alpha stable vector, $\mathbf{X} \stackrel{d}{=} \left\{\mathbf{A}^{\frac{1}{2}}\mathbf{G}_{1,I}, \mathbf{A}^{\frac{1}{2}}\mathbf{G}_{1,Q}, \cdots, \mathbf{A}^{\frac{1}{2}}\mathbf{G}_{d,I}, \mathbf{A}^{\frac{1}{2}}\mathbf{G}_{d,Q}\right\}$ where $\mathbf{A}$ is a positive stable random variable and $\mathbf{G}_{1,I}, \mathbf{G}_{1,Q}, \cdots, \mathbf{G}_{d,I}, \mathbf{G}_{d,Q}$ are *i.i.d.* Gaussian random variables [18], we have

$$\lim_{\beta\to\infty} \beta^{\alpha}\mathbf{P}\left(\|\mathbf{X}_1\| > \beta_1, \cdots, \|\mathbf{X}_d\| > \beta_d\right)$$
$$= \lim_{\beta\to\infty} \beta^{\alpha}\mathbf{P}\left(\mathbf{A}\min_{i=1,\cdots,d}\frac{\beta^2}{\beta_i^2}\left(\mathbf{G}_{i,I}^2 + \mathbf{G}_{i,Q}^2\right) > \beta^2\right) \quad (47)$$
$$= \lim_{\beta\to\infty} \beta^{\alpha}\int_0^{\infty}\mathbb{P}\left(\mathbf{A} > \frac{\beta^2}{x}\right)\frac{1}{2}e^{-\frac{x}{2}}dx \quad (48)$$
$$= 2^{\alpha}\sigma C_{\frac{\alpha}{2}}\cos\left(\frac{\pi\alpha}{4}\right)\Gamma\left(1+\frac{\alpha}{2}\right) \quad (49)$$

where (48) is expressed by noting that for all i, $\frac{\beta_i^2}{\beta^2}\left(\mathbf{G}_{i,I}^2 + \mathbf{G}_{i,Q}^2\right)$ are independent and exponentially distributed with mean $\frac{2\beta^2}{\beta_i^2}$. Thus $\min_{i=1,\cdots,d}\frac{\beta_i^2}{\beta^2}\left(\mathbf{G}_{i,I}^2 + \mathbf{G}_{i,Q}^2\right)$ is also exponentially distributed with mean $\left(\frac{\sum_{i=1}^{d}\beta_i^2}{2\beta^2}\right)^{-1} = 2$. Equation (49) follows from the dominated convergence theorem, and noting that $\mathbf{A}$ is a positive $\frac{\alpha}{2}$-stable random variable with tails $\lim_{t\to\infty} t^{\frac{\alpha}{2}}\mathbb{P}\left(\mathbf{A} > t\right) = 2^{\frac{\alpha}{2}}\sigma C_{\frac{\alpha}{2}}\cos\left(\frac{\pi\alpha}{4}\right)$. ∎

Deriving the joint amplitude tail probability of a general symmetric alpha stable vector is more involved as compared to the specialized case of *isotropic* symmetric alpha stable vector dealt in Theorem A.1. We now prove a theorem which relates the joint amplitude tail probability of a general symmetric alpha stable vector to its spectral measure.

Theorem A.2. *Let $\mathbf{X} = (\mathbf{X}_{1,I}, \mathbf{X}_{1,Q}, \cdots, \mathbf{X}_{d,I}, \mathbf{X}_{d,Q})$ be a symmetric alpha stable vector in $\mathbb{R}^{2d}$ with $0 < \alpha < 2$ and a unique symmetric finite measure $\overline{\Gamma}$ on the unit sphere S_{2d}. If $\beta_i = \beta\eta_i$ such that $0 < \eta_i < \infty$ for $i = 1, \cdots, d$, then*

$$\lim_{\beta\to\infty} \beta^{\alpha}\mathbb{P}\left(\|\mathbf{X}_1\| > \beta_1, \cdots, \|\mathbf{X}_d\| > \beta_d\right) = C_{\alpha}\int_{S_{2d}}\min_{i=1,\cdots,d}\left(\eta_i^{-1}\sqrt{s_{2i-1}^2 + s_{2i}^2}\right)^{\alpha}\overline{\Gamma}(d\mathbf{s}) \quad (50)$$

where C_{α} is defined in (46).

Proof: This proof adopts the approach used in the proof of Theorem 4.4.1 in [18]. Using Theorems 3.5.6 and 3.10.1, and Corollary 3.10.4 in [18],

$$(\mathbf{X}_{1,I}, \mathbf{X}_{1,Q}, \cdots, \mathbf{X}_{d,I}, \mathbf{X}_{d,Q}) \stackrel{d}{=} (\mathbf{Y}_1, \cdots, \mathbf{Y}_{2d}) \quad (51)$$

such that $\mathbf{Y}_k$ have a Le-Page series representation

$$\mathbf{Y}_k = \left(C_{\alpha}\widetilde{\Gamma}(S_{2d})\right)^{\frac{1}{\alpha}}\sum_{i=1}^{\infty}\boldsymbol{\epsilon}_i\boldsymbol{\Gamma}_i^{-\frac{1}{\alpha}}\frac{f_k(\mathbf{V}_i)}{f^*(\mathbf{V}_i)} \quad (52)$$
$$= \underbrace{\left(C_{\alpha}\widetilde{\Gamma}(S_{2d})\right)^{\frac{1}{\alpha}}\boldsymbol{\epsilon}_1\boldsymbol{\Gamma}_1^{-\frac{1}{\alpha}}\frac{f_k(\mathbf{V}_1)}{f^*(\mathbf{V}_1)}}_{\mathbf{U}_k} + \underbrace{\left(C_{\alpha}\widetilde{\Gamma}(S_{2d})\right)^{\frac{1}{\alpha}}\sum_{i=2}^{\infty}\boldsymbol{\epsilon}_i\boldsymbol{\Gamma}_i^{-\frac{1}{\alpha}}\frac{f_k(\mathbf{V}_i)}{f^*(\mathbf{V}_i)}}_{\mathbf{W}_k} \quad (53)$$

Here $f_k : S_{2d} \to \mathbb{R}$ is defined as $f_k(s) = s_k$ for $k = 1, \cdots, 2d$ and $s \in S_{2d}$, $f^* : S_{2d} \to \mathbb{R}$ is defined as $f^*(s) = \max_{k=1,\cdots,2d}|f_k(s)|$ for $s \in S_{2d}$, $\widetilde{\Gamma}(d\mathbf{s}) = (f^*(s))^{\alpha}\overline{\Gamma}(d\mathbf{s})$ is a finite measure on (S_{2d}, Borel σ-algebra on S_{2d}), $\{\boldsymbol{\Gamma}_1, \boldsymbol{\Gamma}_2, \cdots\}$ is the sequence of arrival times of a Poisson process with unit arrival rate, $\{\mathbf{V}_1, \mathbf{V}_2, \cdots\}$ is the sequence independent of $\{\boldsymbol{\Gamma}_1, \boldsymbol{\Gamma}_2, \cdots\}$ such that $\mathbf{V}_i$ has a distribution $\frac{\widetilde{\Gamma}}{\widetilde{\Gamma}(S_{2d})}$ on S_{2d}, and $\{\boldsymbol{\epsilon}_1, \boldsymbol{\epsilon}_2, \cdots\}$ is the sequence independent of $\{\boldsymbol{\Gamma}_1, \boldsymbol{\Gamma}_2, \cdots\}$ and $\{\mathbf{V}_1, \mathbf{V}_2, \cdots\}$ such that $\mathbb{P}(\boldsymbol{\epsilon}_i = 1) = \mathbb{P}(\boldsymbol{\epsilon}_i = -1) = \frac{1}{2}$. Let $\overline{\mathbf{U}} = \min_{i=1,\cdots,d}\frac{\sqrt{\mathbf{U}_{2i-1}^2 + \mathbf{U}_{2i}^2}}{\eta_i}$ and $\overline{\mathbf{W}} = \frac{\max_{i=1,\cdots,2d}|\mathbf{W}_i|}{\min_{i=1,\cdots,d}\eta_i}$.

Using (53), and the triangle inequality, we have

$$\overline{\mathbf{U}} + 2\overline{\mathbf{W}} \leq \min_{i=1,\cdots,d}\frac{\sqrt{\mathbf{Y}_{2i-1}^2 + \mathbf{Y}_{2i}^2}}{\eta_i} \leq \overline{\mathbf{U}} - 2\overline{\mathbf{W}}. \quad (54)$$

Tails of the random variable $\overline{\mathbf{U}}$ can be expressed as

$$\lim_{\beta\to\infty}\beta^{\alpha}\mathbb{P}\left(\overline{\mathbf{U}}>\beta\right)$$

$$=\lim_{\beta\to\infty}\beta^{\alpha}\mathbb{P}\Bigg(\left(C_{\alpha}\widetilde{\Gamma}(S_{2d})\right)^{\frac{1}{\alpha}}\boldsymbol{\Gamma}_1^{-\frac{1}{\alpha}}\times \min_{i=1,\cdots,d}\frac{\sqrt{f_{2i-1}^2(\mathbf{V}_1)+f_{2i}^2(\mathbf{V}_1)}}{\eta_i f^*(\mathbf{V}_1)}>\beta\Bigg) \quad (55)$$

$$=\lim_{\beta\to\infty}\beta^{\alpha}\int_{S_{2d}}\mathbb{P}\Bigg(\left(C_{\alpha}\widetilde{\Gamma}(S_{2d})\right)^{\frac{1}{\alpha}}\boldsymbol{\Gamma}_1^{-\frac{1}{\alpha}}\times \min_{i=1,\cdots,d}\frac{\sqrt{f_{2i-1}^2(s)+f_{2i}^2(s)}}{\eta_i f^*(s)}>\beta\Bigg)\frac{\widetilde{\Gamma}(d\mathbf{s})}{\widetilde{\Gamma}(S_{2d})} \quad (56)$$

$$=\lim_{\beta\to\infty}\beta^{\alpha}\int_{S_{2d}}\left(1-\exp\left(-C_{\alpha}\widetilde{\Gamma}(S_{2d})\beta^{-\alpha}\times \left(\min_{i=1,\cdots,d}\frac{\sqrt{s_{2i-1}^2+s_{2i}^2}}{\eta_i f^*(s)}\right)^{\alpha}\right)\right)\frac{\widetilde{\Gamma}(d\mathbf{s})}{\widetilde{\Gamma}(S_{2d})} \quad (57)$$

$$=C_{\alpha}\int_{S_{2d}}\min_{i=1,\cdots,d}\left(\eta_i^{-1}\sqrt{s_{2i-1}^2+s_{2i}^2}\right)^{\alpha}\overline{\Gamma}(d\mathbf{s}) \quad (58)$$

where (56) involves integrating over the distribution of $\mathbf{V}_1$, and (58) is derived using the dominated convergence theorem and transforming the finite measure over which the integral is expressed. From (58), it can be noted that the random variable $\overline{\mathbf{U}}$ is regularly varying (as defined by in Lemma 4.4.2 in [18]). Furthermore, $\overline{\mathbf{W}}$ is a positive random variable and the relation $\lim_{\beta\to\infty}\beta^{\alpha}\mathbb{P}\left(\max_{i=1,\cdots,2d}|\mathbf{W}_i|>\beta\right)=0$ was proved as an intermediate step in the proof of Theorem 4.4.1 in [18]. Using Lemma 4.4.2 in [18], the tails of $\overline{\mathbf{U}}\pm 2\overline{\mathbf{W}}$ are dominated by the tails of $\overline{\mathbf{U}}$. Using (50), (54), and Lemma 4.4.2 in [18],

$$\lim_{\beta\to\infty}\beta^{\alpha}\mathbb{P}\left(\|\mathbf{X}_1\|>\beta_1,\cdots,\|\mathbf{X}_d\|>\beta_d\right)$$

$$=\lim_{\beta\to\infty}\beta^{\alpha}\mathbb{P}\left(\min_{i=1,\cdots,d}\frac{\sqrt{\mathbf{Y}_{2i-1}^2+\mathbf{Y}_{2i}^2}}{\eta_i}>\beta\right) \quad (59)$$

$$=\lim_{\beta\to\infty}\beta^{\alpha}\mathbb{P}\left(\overline{\mathbf{U}}>\beta\right) \quad (60)$$

$$=C_{\alpha}\int_{S_{2d}}\min_{i=1,\cdots,d}\left(\eta_i^{-1}\sqrt{s_{2i-1}^2+s_{2i}^2}\right)^{\alpha}\overline{\Gamma}(d\mathbf{s}). \quad (61)$$

This concludes the proof of the theorem. ∎

Using Theorem A.2, we now prove a result which is relevant for the particular form of the symmetric alpha stable vectors derived in this paper.

Corollary A.2.1. *Let $\mathbf{X}=(\mathbf{X}_{1,I},\mathbf{X}_{1,Q},\cdots,\mathbf{X}_{d,I},\mathbf{X}_{d,Q})$ be a symmetric alpha stable vector in $\mathbb{R}^{2d}$ with $0<\alpha<2$ and a spectral measure $\overline{\Gamma}$ on the unit sphere S_{2d}. Consider the case when the spectral measure is a sum of independent spectral measures of the form*

$$\overline{\Gamma}=\overline{\Gamma}_0+\sum_{k=1}^{|\mathcal{X}|}\overline{\Gamma}_k\delta\left(\bigcup_{j\in\mathcal{X}(k)}\{s_{2j-1},s_{2j}\}\right) \quad (62)$$

where $\mathcal{X}$ is an arbitrary collection of non-empty proper subsets of $\{1,2,\cdots,n\}$, $|\mathcal{X}|$ denotes the cardinality of $\mathcal{X}$, $\mathcal{X}(k)$ is the k^{th} set contained in $\mathcal{X}$, $\delta(\cdots)$ denotes the dirac delta functional, $\overline{\Gamma}_0$ is a spectral measure distributed over the unit sphere S_{2n}, and $\overline{\Gamma}_k$ is a spectral measure distributed over $S_{2(n-|\mathcal{X}(k)|)}$ formed from the dimensions $\cup_{j=1,\cdots,2n;j\notin\mathcal{X}(k)}\{2j-1,2j\}$. If $\beta_i=\beta\eta_i$ such that $0<\eta_i<\infty$ for $i=1,\cdots,d$, then the joint tail probability are dominated by the spectral measure $\overline{\Gamma}_0$ such that

$$\lim_{\beta\to\infty}\beta^{\alpha}\mathbb{P}\left(\|\mathbf{X}_1\|>\beta_1,\cdots,\|\mathbf{X}_d\|>\beta_d\right) =C_{\alpha}\int_{S_{2d}}\min_{i=1,\cdots,d}\left(\eta_i^{-1}\sqrt{s_{2i-1}^2+s_{2i}^2}\right)^{\alpha}\overline{\Gamma}_0(d\mathbf{s}). \quad (63)$$

Proof:

$$\lim_{\beta\to\infty}\beta^{\alpha}\mathbb{P}\left(\|\mathbf{X}_1\|>\beta_1,\cdots,\|\mathbf{X}_d\|>\beta_d\right)$$

$$=C_{\alpha}\Bigg[\int_{S_{2d}}\min_{i=1,\cdots,d}\left(\eta_i^{-1}\sqrt{s_{2i-1}^2+s_{2i}^2}\right)^{\alpha}\overline{\Gamma}_0(d\mathbf{s})+\sum_{k=1}^{|\mathcal{X}|}\int_{S_{2d}}\min_{i=1,\cdots,d}\left(\eta_i^{-1}\sqrt{s_{2i-1}^2+s_{2i}^2}\right)^{\alpha}\times\delta\left(\bigcup_{j\in\mathcal{X}(k)}\{s_{2j-1},s_{2j}\}\right)\overline{\Gamma}_k(d\mathbf{s})\Bigg] \quad (64)$$

$$=C_{\alpha}\int_{S_{2d}}\min_{i=1,\cdots,d}\left(\eta_i^{-1}\sqrt{s_{2i-1}^2+s_{2i}^2}\right)^{\alpha}\overline{\Gamma}_0(d\mathbf{s}) \quad (65)$$

since $\min_{i=1,\cdots,d}\left(\eta_i^{-1}\sqrt{s_{2i-1}^2+s_{2i}^2}\right)^{\alpha}\delta\Big(\bigcup_{j\in\mathcal{X}(k)}\{s_{2j-1},s_{2j}\}\Big)=0$ as $\mathcal{X}(k)$ is a non-empty set. ∎

REFERENCES

[1] K. Gulati, "*Radio Frequency Interference Modeling and Mitigation in Wireless Receivers*," Ph.D. dissertation, The University of Texas at Austin, Aug. 2011. [Online]. Available: http://users.ece.utexas.edu/~bevans/students/phd/kapil_gulati/

[2] F. Baccelli and B. Błaszczyszyn, "Stochastic geometry and wireless networks, volume 2— applications," in *Foundations and Trends in Networking*. Now Publishers Inc., March 2009, vol. 4, no. 1–2, pp. 1–312.

[3] M. Haenggi and R. K. Ganti, "Interference in large wireless networks," in *Foundations and Trends in Networking*. Now Publishers Inc., Dec. 2008, vol. 3, no. 2, pp. 127–248.

[4] S. Weber, J. G. Andrews, and N. Jindal, "An overview of the transmission capacity of wireless networks," *IEEE Transactions on Communications*, vol. 58, no. 12, pp. 3593–3604, Dec. 2010.

[5] M. Haenggi, "Local delay in static and highly mobile Poisson networks with ALOHA," in *Proc. IEEE International Conference on Communications*, Cape Town, South Africa, May 23–27 2010, pp. 1–5.

[6] F. Baccelli and B. Błaszczyszyn, "A new phase transition for local delays in MANETs," in *Proc. IEEE International Conference on Computer Communications*, San Diego, CA, Mar. 14–19 2010, pp. 1–9.

[7] R. K. Ganti and M. Haenggi, "Spatial and temporal correlation of the interference in ALOHA ad hoc networks," *IEEE Communications Letters*, vol. 13, no. 9, pp. 631–633, Sep. 2009.

[8] S. Weber, X. Yang, J. G. Andrews, and G. de Veciana, "Transmission capacity of wireless ad hoc networks with outage constraints," *IEEE Transactions on Information Theory*, vol. 51, no. 12, pp. 4091–4102, Dec. 2005.

[9] F. Baccelli and B. Błaszczyszyn, "Stochastic geometry and wireless networks, volume 1 — theory," in *Foundations and Trends in Networking*. Now Publishers Inc., March 2009, vol. 3, no. 3–4, pp. 249–449.

[10] K. Gulati, B. L. Evans, J. G. Andrews, and K. R. Tinsley, "Statistics of co-channel interference in a field of Poisson and Poisson-Poisson clustered interferers," *IEEE Transactions on Signal Processing*, vol. 58, no. 12, pp. 6207–6222, Dec. 2010.

[11] E. S. Sousa, "Performance of a spread spectrum packet radio network link in a Poisson field of interferers," *IEEE Transactions on Information Theory*, vol. 38, no. 6, pp. 1743–1754, Nov. 1992.

[12] S. B. Lowen and M. C. Teich, "Power-law shot noise," *IEEE Transactions on Information Theory*, vol. 36, no. 6, pp. 1302–1318, Nov. 1990.

[13] J. Ilow and D. Hatzinakos, "Analytic alpha-stable noise modeling in a Poisson field of interferers or scatterers," *IEEE Transactions on Signal Processing*, vol. 46, no. 6, pp. 1601–1611, Jun. 1998.

[14] X. Yang and A. Petropulu, "Co-channel interference modeling and analysis in a Poisson field of interferers in wireless communications," *IEEE Transactions on Signal Processing*, vol. 51, no. 1, pp. 64–76, Jan. 2003.

[15] M. Z. Win, P. C. Pinto, and L. A. Shepp, "A mathematical theory of network interference and its applications," *Proceedings of the IEEE*, vol. 97, no. 2, pp. 205–230, Feb. 2009.

[16] P. Cardieri, "Modeling interference in wireless ad hoc networks," *IEEE Communications Surveys & Tutorials*, vol. 12, no. 4, pp. 551–572, Fourth Quarter 2010.

[17] D. Middleton, "Statistical–physical models of man–made and natural radio noise part II: First order probability models of the envelope and phase," U.S. Department of Commerce, Office of Telecommunications, Tech. Rep., Apr. 1976.

[18] G. Samorodnitsky and M. S. Taqqu, *Stable Non-Gaussian Random Processes: Stochastic Models with Infinite Variance*. Chapman and Hall, New York, 1994.

[19] J. G. Andrews, S. Weber, M. Kountouris, and M. Haenggi, "Random access transport capacity," *IEEE Transactions On Wireless Communications*, vol. 9, no. 6, pp. 2101–2111, Jun. 2010.

[20] R. Vaze, "Throughput-delay-reliability tradeoff in ad hoc networks," in *Proc. Workshop on Spatial Stochastic Models for Wireless Networks*, Avignon, May 31 – Jun. 4 2010, pp. 459–464.

[21] R. Baldick, *Applied Optimization: Formulation and Algorithms for Engineering Systems*. Cambridge University Press, 2006.

[22] A. Spaulding and D. Middleton, "Optimum reception in an impulsive interference enviroment-part I: Coherent detection," *IEEE Transactions on Communications*, vol. 25, no. 9, pp. 910–923, 1977.

[23] M. Nassar, K. Gulati, M. DeYoung, B. L. Evans, and K. R. Tinsley, "Mitigating near-field interference in laptop embedded wireless transceivers," *Journal of Signal Processing Systems*, Mar. 2009. [Online]. Available: http://dx.doi.org/10.1007/s11265-009-0350-7

[24] K. Gulati, M. Nassar, A. Chopra, N. B. Okafor, M. DeYoung, N. Aghasadeghi, A. Sujeeth, and B. L. Evans, "Radio frequency interference modeling and mitigation toolbox in MATLAB," Version 1.6, Apr. 2011. [Online]. Available: http://users.ece.utexas.edu/~bevans/projects/rfi/software/

[25] F. Baccelli, B. Błaszczyszyn, and P. Muhlethaler, "An Aloha protocol for multihop mobile wireless networks," *IEEE Transaction on Information Theory*, vol. 52, no. 2, pp. 412–436, Sep. 2006.

[26] A. Hasan and J. G. Andrews, "The guard zone in wireless ad hoc networks," *IEEE Transactions on Wireless Communications*, vol. 4, no. 3, pp. 897–906, Mar. 2007.

Kapil Gulati (S'06 M'12) received the B.Tech. degree in Electronics and Communications Engineering from the Indian Institute of Technology, Guwahati in 2004 and the M.S. and Ph.D. degree in Electrical Engineering from the University of Texas at Austin in 2008 and 2011, respectively. From 2004 to 2006, he was employed as a Hardware Design Engineer at Texas Instruments, India. Since 2011, he has been employed as a Senior Systems Engineer at Qualcomm Incorporated, San Diego, CA.

Radha Krishna Ganti (S'01, M'10) is an Assistant Professor at the Indian Institute of Technology Madras, Chennai, India. He was a Postdoctoral researcher in the Wireless Networking and Communications Group at UT Austin from 2009-2011. He received his B. Tech. and M. Tech. in EE from the Indian Institute of Technology, Madras, and a Masters in Applied Mathematics and a Ph.D. in EE from the University of Notre Dame in 2009. His doctoral work focused on the spatial analysis of interference networks using tools from stochastic geometry. He is a co-author of the monograph Interference in Large Wireless Networks (NOW Publishers, 2008).

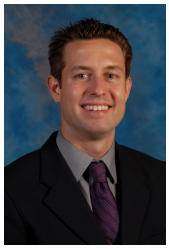

Jeffrey Andrews (S'98, M'02, SM'06) received the B.S. in Engineering with High Distinction from Harvey Mudd College in 1995, and the M.S. and Ph.D. in Electrical Engineering from Stanford University in 1999 and 2002, respectively. He is a Professor in the Department of Electrical and Computer Engineering at the University of Texas at Austin, where he was the Director of the Wireless Networking and Communications Group (WNCG) from 2008-12. He developed Code Division Multiple Access systems at Qualcomm from 1995-97, and has consulted for entities including the WiMAX Forum, Microsoft, Apple, Clearwire, Palm, Sprint, ADC, and NASA.

Dr. Andrews is co-author of two books, *Fundamentals of WiMAX* (Prentice-Hall, 2007) and *Fundamentals of LTE* (Prentice-Hall, 2010), and holds the Earl and Margaret Brasfield Endowed Fellowship in Engineering at UT Austin, where he received the ECE department's first annual High Gain award for excellence in research. He is a Senior Member of the IEEE, a Distinguished Lecturer for the IEEE Vehicular Technology Society, served as an associate editor for the *IEEE Transactions on Wireless Communications* from 2004-08, was the Chair of the 2010 IEEE Communication Theory Workshop, and is the Technical Program co-Chair of ICC 2012 (Comm. Theory Symposium) and Globecom 2014. He has also been a guest editor for two recent *IEEE JSAC* special issues on stochastic geometry and femtocell networks.

Dr. Andrews received the National Science Foundation CAREER award in 2007 and has been co-author of five best paper award recipients, two at Globecom (2006 and 2009), Asilomar (2008), the 2010 IEEE Communications Society Best Tutorial Paper Award, and the 2011 Communications Society Heinrich Hertz Prize. His research interests are in communication theory, information theory, and stochastic geometry applied to wireless cellular and ad hoc networks.

Brian L. Evans (S'87, M'93, SM'97, F'09) is the Engineering Foundation Professor of Electrical and Computer Engineering at The University of Texas at Austin. He earned a BSEECS (1987) degree from the Rose-Hulman Institute of Technology, and MSEE (1988) and PhDEE (1993) degrees from the Georgia Institute of Technology. From 1993 to 1996, he was a post-doctoral researcher at the University of California, Berkeley.

Prof. Evans develops signal processing theory and algorithms with implementation constraints in mind, and translates algorithms into design methods, embedded prototypes and full system testbeds. He is currently researching interference mitigation in communication systems, rolling shutter artifact mitigation in video acquisition, and system-level reliability for multicore embedded systems.

He has published 200+ refereed conference and journal papers, and graduated 20 PhD students. He received several UT Austin teaching awards: ECE Lepley (2008), Texas Exes (2011) and IEEE/HKN Chapter Best Professor (2012). He received a 1997 US NSF CAREER Award.

Srikathyayani Srikanteswara is a Sr. Research Scientist at Intel Labs, where she leads research on cognitive radios and spectrum sharing techniques. She has been involved in shaping research on simultaneous operation of radios as well as developing and prototyping spectrum sensing algorithms. Prior to joining Intel, she was with Navsys Corporation, and Virginia Tech, where she was a research faculty member with the Mobile and Portable Radio Research Group (MPRG), where she developed Software Defined Radio (SDR) architectures for mobile platforms and DSP algorithms for communications. Her research interests include cognitive radios, multi radio interference mitigation, and spectrum sensing. She received her BS with Honors in Electrical Engineering from IT-BHU, India. She received MS and Ph.D. from Virginia Tech in 1997 and 2001 respectively.